universität wien

MASTERARBEIT / MASTER'S THESIS

Titel der Masterarbeit / Title of the Master's Thesis

„Anticancer activity of *Curcuma longa* and affected signaling pathways in prostate cancer cells“

verfasst von / submitted by

Tianchi Jiang, BSc

angestrebter akademischer Grad / in partial fulfilment of the requirements for the degree of

Master of Science (MSc)

Wien, 2022 / Vienna, 2022

Studienkennzahl lt. Studienblatt / degree programme code as it appears on the student record sheet:	UA 066 830
Studienrichtung lt. Studienblatt / degree programme as it appears on the student record sheet:	Molecular Microbiology, Microbial Ecology and Immunobiology
Betreut von / Supervisor:	Assoc. Prof. Priv.-Doz. Dr. Yan Ma

Acknowledgement

I would like to express my sincere gratitude to a lot of people, without whom I would not be able to finish this thesis.

First, I am deeply grateful to Assoc. Prof. Priv.-Doz. Dr. Yan Ma for her constant guidance, support, and advice throughout my research work. I would also like to express my sincere thankfulness to Dr. Johannes Jakowitsch for his great support.

I am also very thankful to all the other lab members: Shan He, PhD, Dr. Amar Saciri, and Winnie Xiao, MSc, for the help and advice I sometimes urgently needed, and for the learning and discussion time I greatly enjoyed.

Lastly, I would like to thank my friend Alex Chun Wai Wong, BSc, for his help and advice in the bioinformatic analyses.

Table of Contents

Abstract

Prostate cancer (PCa) is among the most common malignancies in males worldwide. Low specificity in diagnosis and diverse levels of limitations in current therapeutic options have been reported. Therefore, alternative and complementary therapies that demonstrate efficacy and safety in PCa treatment are crucially demanded. The medicinal herb *Curcuma longa* has been reported to have anticancer effects. This study aims to evaluate the anti-cancer activity of *C. longa* in human PCa cells, to understand the mechanisms involved, and to discover potential biomarkers for the early diagnosis and treatment of PCa.

Stability tests and quality control assessments of the purified *C. longa* extract were conducted. We performed cell viability assay on the human PCa cell lines DU145, PC3, and the prostate epithelial cell line PNT2, followed by FACS-based apoptosis detections. Quantitative real-time PCR and western blot analysis were used to quantify the expression levels of different cancer-related genes. In addition, Illumina RNA sequencing and subsequent bioinformatic analysis of gene expression profiles and signaling pathways were performed.

Our data suggest that *C. longa* inhibited the cell viability of the PCa cell lines DU145 and PC3, and induced cell apoptosis. The expression of the tumor suppressor p21, and the PCa-specific genes TMEM79 and ACOXL were significantly up-regulated in both RNA and protein levels. An up-regulation of diverse tumor suppressors and a down-regulation of multiple tumor-promoting genes were detected through the RNA sequencing. Furthermore, various cancer-related signaling pathways were dysregulated after the *C. longa* treatment.

Conclusively, *C. longa* inhibited cell viability, induced apoptosis and dysregulated multiple cancer-related genes in PCa cells, indicating the efficacy of *C. longa* in the treatment of PCa. Moreover, TMEM79 and ACOXL could be putative biomarker candidates for the early diagnosis and therapy of PCa.

Key words: Anticancer activity, *Curcuma longa,* herbal medicine, signaling pathways, prostate cancer cells

Zusammenfassung

Prostatakrebs (PCa) gehört weltweit zu den häufigsten bösartigen Tumoren bei Männern. Vielfach wird über eine geringe Spezifität bei der Diagnose und verschiedene Grade von Einschränkungen bei den derzeitigen therapeutischen Optionen berichtet. Daher besteht ein dringender Bedarf an alternativen und komplementären Therapien mit Wirksamkeit und Sicherheit bei der PCa-Behandlung. Dem Heilkraut *Curcuma longa* wird eine krebshemmende Wirkung nachgesagt. Diese Studie zielt darauf ab, die krebshemmende Aktivität von *C. longa* in menschlichen PCa-Zellen zu bewerten, die beteiligten Mechanismen zu verstehen und potenzielle Biomarker für die frühe Diagnose und Behandlung von PCa zu entdecken.

Es wurden Stabilitätstests und Qualitätskontrollen des gereinigten *C. longa*-Extrakts durchgeführt. Wir führten einen Zellviabilitäts-Assay an den menschlichen PCa-Zelllinien DU145, PC3 und der Prostata-Epithelzelllinie PNT2 durch, gefolgt von FACS-basierter Apoptose-Detektion. Quantitative Real-Time PCR und Western-Blot-Analysen wurden unternommen, um die Expressionsniveaus verschiedener krebsbezogener Gene zu quantifizieren. Zusätzlich wurden eine Illumina-RNA-Sequenzierung samt anschließender bioinformatischer Analyse von Genexpressionsprofilen und Signalwegen durchgeführt.

Unsere Daten legen nahe, dass *C. longa* die Viabilität der PCa-Zelllinien DU145 und PC3 hemmte und die Zellapoptose induzierte. Die Expression des Tumorsuppressors p21 und der PCa-spezifischen Gene TMEM79 und ACOXL waren sowohl auf RNA- als auch auf Proteinebene signifikant hochreguliert. Durch die RNA-Sequenzierung wurde eine Hochregulation diverser Tumorsuppressoren und eine Herunterregulation mehrerer tumorfördernder Gene nachgewiesen. Darüber hinaus waren verschiedene krebsrelevante Signalwege nach der Behandlung mit *C. longa* fehlreguliert.

Zusammenfassend hemmte *C. longa* die Zellviabilität, induzierte die zelluläre Apoptose und dysregulierte mehrere krebsrelevante Gene in PCa-Zellen, was auf eine mögliche Wirksamkeit von *C. longa* bei der Behandlung von PCa hinweist. Darüber hinaus könnten TMEM79 und ACOXL mutmaßliche Biomarkerkandidaten für die Früherkennung und Therapie von PCa darstellen.

Stichwörter: Antikrebsaktivität, *Curcuma longa*, Kräutermedizin, Signalwege, Prostatakrebszellen

Abbreviation

ACOXL	Acyl-coenzyme A oxidase-like protein
ACTs	Artemisinin-based combination treatment
ADT	androgen deprivation therapy
AKR1C2	Aldo-Keto reductase 1C2
AP1	activating protein-1
AR	androgen receptor
AS	active surveillance
BP	biological process
BPH	benign prostatic hypertrophy
CC	cellular component
CDKs	cyclin dependent kinases
CL	Curcuma longa
CRPC	castration-resistant prostate cancer
CTLA-4	cytotoxic T-lymphocyte antigen
CYP	cytochrome P
CYR61	cysteine-rich angiogenic inducer 61
DBD	DNA-binding domain
DKK1	Dickkopf 1
DRE	digital rectal exam
ECM	extracellular matrix
ER	estrogen receptor
FOSL1	Fos-like gene 1
GO	gene ontology
GR	glucocorticoid receptor
GSEA	Gene Set Enrichment Analysis
GSTP1	glutathione S-transferase
HLH	helix-loop-helix
HPLC	High Performance Liquid Chromatography
INSIG1	insulin-induced gene 1
IPA	Ingenuity Pathway Analysis
LBD	ligand-binding domain
LHRH	leuteinizing hormone-releasing hormone
LUTS	lower urinary tract symptoms
mCRPC	metastatic castration-resistant prostate cancer
MF	molecular function
MSigDB	Molecular Signatures Database

NCOA2	nuclear receptor coactivator
NDRG1	N-myc downregulated gene 1
NFκB	nuclear factor-κB
NTD	N-terminal domain
ODC1	ornithine decarboxylase
p21	cyclin-dependent kinase inhibitor p21
p53	tumor protein 53
PBS	phosphate-buffered saline
PCa	prostate cancer
PCNA	proliferating cell nuclear antigen
PDXs	patient-derived xenografts
PI	propidium iodic
PIK3CG	phosphatidylinositol-4,5-bisphosphate 3-kinase
PIN	prostatic intraepithelial neoplasia
PKB	protein kinase B
PR	progesterone receptor
PSA	Prostate Specific Antigen
RT	room temperature
SD	standard deviations
SRC	steroid receptor coactivator family
TCM	Traditional Chinese Medicine
TCMSP	Traditional Chinese Medicine Systems Pharmacology Database and Analysis Platform
TNFα	tumor necrosis factor-alpha
TRAMP	transgenic adenocarcinoma mouse prostate
TRUS	transperineal or transrectal
UPP1	uridine phosphorylase 1

1 Introduction

With 1.2 million new cases in 2019, prostate cancer (PCa) is currently one of the most common malignancies, and a leading cause of cancer mortality in males worldwide. In Austria and Germany, PCa has been reported to have the highest in-patient discharge rates among men [1, 2]. Modern diagnosis and treatment of PCa include screening trial, prostate specific antigen (PSA) testing, advanced functional imaging, hormone manipulation, surgery, chemotherapy and radiotherapy. The wide variety of diagnostic and therapeutic options mainly depend on the clinical scenario and the risk category of the patient [3, 4]. However, limitations and adverse effects have been reported [5, 6, 7, 8]. PSA tests might potentially results in over-diagnosis and consequently overtreatment, due to its low specificity [5, 6]. All aggressive therapies for PCa have the possibility to cause erectile dysfunction and urinary incontinence [7, 8]. Recurrences from chemotherapy and resistance to chemotherapy are the leading causes of drug failure upon metastasis [9]. With the progress of the disease, patients with metastatic PCa are highly likely to become resistant to androgen suppression, the mortality of the patients significantly increase once entering the castration-resistant state [9, 10]. Therefore, novel biomarkers, as well as new alternative and complementary therapies that demonstrate efficacy in PCa treatment with less associated side effects, are still in urgent need. Research on novel therapeutic opportunities continues to attempt to prolong survival and improve quality of life.

Chinese medicinal herbs embrace a cocktail of diverse bioactive compounds, mainly in the roots, leaves and stems of the plant [11]. The anticancer effects of different Chinese herbal medicine and medicinal herbs have nowadays been actively evaluated [2].

Curcuma longa is a medicinal herb that belongs to the ginger family. The most commonly used part of the plant is the dried rhizome, which has a long history of being used as herbs, spice and colorant in China and other Asian countries [12, 13]. *C. longa* and its main chemical compounds have been reported to present anticancer effect on different types of cancer, by modulating different molecular regulators and interfering with various signaling pathways [12, 13, 14].

2 Background

2.1 Clinical features of PCa

PCa is among the most common cancer in males worldwide. The incidence of PCa is strongly age-related, with the majority of the cases in men aged above 50 and reaches the

peak in men above 90 [15]. Although most of the slow-growing PCa cases are considered to have relatively low risk and are not life-threatened, patients who develop high-risk localized, locally advanced or metastatic cancer is highly possible to become resistant to treatment. Therefore, PCa results in a globally high cancer-related mortality among men [2, 3]

Early PCa barely presents symptoms. Some studies suggested that, most of the symptoms occurred in patients with an early PCa share similarities and have crossover with other abnormalities like prostatitis and benign prostatic hypertrophy (BPH), making it a challenge of distinguishing the diseases only based on the symptoms [15, 16].

However, according to a population-based case-control study in UK, eight pre-diagnostic clinical features, including urinary retention, hesitancy, impotence, frequency, nocturia, haematuria, first and second presentation of weight loss, were independently linked to PCa [16]. Therefore, lower urinary tract symptoms (LUTS) might also be a potential indicator for the early diagnosis of PCa.

With the disease progression, advanced PCa presents more significant symptoms, including blood in the urine or semen, erectile dysfunction, weakness in the lower limbs, and pain in the hips, spine or some other areas of the body [17].

An early diagnosis and treatment of PCa leads to a significantly reduced possibility of tumor progression and metastasis, and is positively linked to an improved survival rate [17].

2.2 Current diagnostic and therapeutic options for PCa

The widespread use of PSA screening in asymptomatic men has contributed to the rising diagnosis of PCa in the last decades, mainly in the United States and many parts of Europe [15]. PSA is a glycoprotein expressed by both normal and neoplastic prostate tissue. The absolute value of PSA in the serum is used as a marker for determining the extent of PCa and evaluating the response of the treatment. Under normal circumstances, PSA is synthesized by secretory cells in the prostate gland into the prostate lumen, where active PSA directly diffuse into the blood circulation, and undergoes proteolytic process to generate inactive PSA. Part of the inactive PSA enters the bloodstream, in an unbound state, which in healthy people reflects the amount of the glandular epithelium, and thus the prostate size. The concentration of the free unbound PSA in the serum is lower in men with prostate cancer, while the complexed amount higher [18]. According to Johns Hopkins Medicine, a range between 1.0 and 1.5 ng/ml is considered normal [19]. However, age, race, body weight and medications are all factors affecting the PSA levels and should be taken into consideration for the determination of the reference ranges [18, 19]. Therefore, the level of PSA below 4.0 ng/ml is

accepted by most doctors as normal [20]. A borderline range of PSA between 2.5 and 10 ng/ml creates a diagnostic conundrum, further diagnostic methods like prostate biopsy and digital rectal exam (DRE) is recommended [18, 20]. Prostate biopsy is currently accepted as the gold standard diagnostic method for PCa after PSA test, via a transperineal or transrectal (TRUS) approach instructed by ultrasound, while DRE enables clinicians to roughly identify the abnormalities of the prostate [21]. In addition, an advanced PSA testing, which includes parameters like PSA density, PSA velocity and free versus complexed or bound PSA would be helpful for the detection and the decision making [18]. The short half-life of PSA and the fact that it could be affected by multiple factors causes the low sensitivity and low specificity of the PSA tests, which might further result in over-diagnosis and overtreatment [5, 6]. Hence, an improvement of the diagnosis accuracy is crucially required.

Once diagnosed, there is a wide range of therapeutic options, either as monotherapy or used in combination, based on the clinical risk category and the condition of the patients, although some remain controversial [3, 4, 7]. Despite the fact that the criteria for the definition of low-risk prostate cancer vary between different institutions, the following attributes are generally accepted: Gleason score ≤ 6/10; serum PSA value ≤ 10 ng/ml; biopsy cores positive for cancer ≤ 30%, negative DRE and ≤ 50% involvement for the positive core containing the most cancer [22]. Based on histological patterns, the Gleason grading system is the most widely used grading system defining PCa aggressiveness [23]. Current treatment options for low-risk prostate cancer include active surveillance (AS), ablative therapies, radiation therapy (RT), and radical prostatectomy [4, 22]. Active surveillance refers to the regular monitoring process of the following index: Gleason score, serum PSA value, serial biopsies, DRE findings and various diagnostic imaging, aiming to provide immediate treatment when the disease progresses, while avoiding overtreatment and adverse impact at the same time [4, 22]. Ablative therapies destroy the cancerous foci on the prostate using energy in a minimally invasive way, and thus provides a compromise between AS and surgery in patients with low-risk PCa [4]. Radiation therapy, a type of treatment using high-energy rays to shrink tumors and kill tumor cells, can be applied to patients receiving both primary and adjuvant therapy. Brachytherapy is usually given to patients with a relative low- to intermediate-risk disease; while external beam, the main delivery method for RT, is given as primary therapy to patients with a locally advanced disease, when radical prostatectomy is no longer an option [4, 24]. The open surgical treatment method for PCa has been widely replaced by the minimally invasive robot-assisted option. For whom surgery is still necessary, radical prostatectomy, the main type of surgery for PCa is mostly suggested as the first step in advanced local, or sometimes even early metastatic disease. In this surgery, the entire prostate gland is removed, along with some of the tissue around it. With the development of therapeutic options for PCa, surgical treatment might be less relevant, while on the other hand, radical prostatectomy might still remain significant for

some patients with a changing indication [4, 7, 25]. According to different statistics, low-risk and slow-growing PCa generally have a relative high survival rate [3, 4, 8].

Androgen-deprivation therapy (ADT), an antihormone therapy based on the crucial role of androgen on the survival and growth of PCa cells, is widely used in advanced, metastatic PCa, aiming to reduce the androgen level and slow down the disease progression by castrating the levels of androgen, mainly testosterone, via pharmaceutical or surgical method, the former being used more frequently these days. The pharmaceutical candidates of ADT to block the androgen receptor (AR) or the synthesis of testosterone include leuteinizing hormone-releasing hormone (LHRH) agonists and antagonists, the inhibitors of cytochrome P (CYP), AR abtagonists, 5α-reductase inhibitors, AR degrading agents and N-terminal AR inhibitors, some of which are still investigational products [3, 4, 27]. Drugs that inhibit 5α-reductase (eg, dutasteride and finasteride) are less aggressive form of ADT, mainly for the primary treatment of BPH [4]; while the CYP inhibitor abiraterone acetate and the AR inhibitor enzalutamide, are proved to have long-lasting survival benefits for metastatic castration-resistant prostate cancer (mCRPC) [3, 4, 26]. ATP can be used either alone or in combination with other therapeutic options, including radiation therapy and chemotherapy, in both cases effective control and an improvement in the overall survival rate have been demonstrated [3, 4, 10]. However, adverse effects have been reported: abiraterone acetate has the possibility of inducing hypertension and cardiac disorders, enzalutamide blocks AR transfer and might cause suppression in agonist-like activities [2]. Additionally, patients have the possibility of developing androgen resistance, leading to a progression of mCRPC and treatment failure in ADT [28].

Chemotherapy and immunotherapy are two other viable options for systemically advanced PCa [4, 29]. Chemotherapy drugs including Docetaxel, a microtubule inhibitor and Cavazitaxl, a tubulin-binding agent are proved to be beneficial for the treatment of mCRPC in randomized studies and clinical trials, and present an improvement in progression-free and survival rate, despite possibility of neutropenia and infection, as well as side effects including headache and muscle weakness being reported [4, 30]. Immunotherapies kill cancer cells by the own immune system of the patients. Current immunotherapy approaches such as cancer vaccines, immune checkpoints and adoptive cellular therapy has presented morphologic changes in clinical trials [4, 29]. Cancer vaccines stimulate the immune system by targeting the PSA with T cells via endogenous T cell receptors, thus inducing the T cell-mediated responses. Immune checkpoints inhibitors enhance immune-mediated antitumor effect by removing signals which block the activation of T cells. Typical immune checkpoints inhibitors are: Cytotoxic T-lymphocyte antigen (CTLA-4), protein PD1 and PD-L1 inhibitors, leading to the restoration of T cells for targeting cancer cells [4, 29]. In spite of recent progress and clinical application,

immunotherapies only present modest efficacy. Side effects, short half-life of the agents and relative low levels of the targeting molecules are limitations to overcome [29].

All aggressive therapies result in distinct levels of adverse effects and dysfunction of neighboring tissues and organs [4, 7]. Furthermore, therapeutic opportunity for mCRPC is crucially limited [3, 26]. Despite current progress in drug development, PCa still remains a significant medical problem, thus novel alternative therapies with promising efficacy and less associated toxicities or side effects are in urgent need.

2.3 Pathological progression of PCa

The pathogeneses and malignances of PCa follows a complicated, multistep process, undergoing the transformation of the following states: normal prostate epithelial, prostatic intraepithelial neoplasia (PIN), localized PCa, invasive adenocarcinoma, primary castration-resistant prostate cancer (CRPC) and mCRPC [23, 31].

Anatomically, the human prostate consists of four zones: a peripheral zone, where around 70% - 80% of PCas arise; a transition zone, which associates with the development of BPH; a central zone and the anterior fibromuscular stroma [23, 31]. Histologically, the prostate is comprised of a stroma compartment and a pseudostratified epithelium, separated by a basement membrane [31]. Three terminally differentiated cells: luminal cells, basal cells and neuroendocrine cells make up the pseudostratified epithelium of the prostate gland and are closely related to different types of carcinogenesis. Luminal cells and basal cells are believed to be the cell of origin, developing adenocarsinoma, neuroendocrine carcinoma and squamous carcinoma, and contribute to the tumorigenesis of PCa, while the link between neuroendocrine cells and PCa remains unclear [23, 31].

Multiple genetic alterations, such as overexpression of oncogenes and conditional inactivation of tumor suppressor genes contribute to the transformation of PCa [23, 31]. The abnormal expression of the gene regulators differs depending on the stages of PCa progression. In the premalignant lesions, overexpression of the anti-apoptotic oncogenic protein BCL2 was reported and suggested to be the key regulator of the progression from normal to malignant PCa. Moreover, an elevated expression of the π-class glutathione S-transferase (GSTP1), the proliferative marker Ki-67, and the protooncogene MYC; as well as a decreased expression of the cyclin-dependent kinase inhibitor p27, TMPRSS2-ERG fusion gene, NKX3.1 and SPOP were observed in the high grade PIN, contributing to the early events of the PCa development. During the transformation from PIN to carcinoma, the loss of RB1, PTEN and an activation of telomerase plays critical roles. Overexpression of numerous oncogenes including CXR4,

EZH2, cMYB, ATM, RAD51 leads to the activation of multiple oncogenic pathways and are reported to be crucially related to the PCa progression towards metastatic stage [23, 31, 32].

Due to the androgen dependence of PCa cells, AR plays a crucial role in the pathogenesis of PCa [3, 31]. AR share structural similarities with other steroid receptors, like estrogen receptor (ER), glucocorticoid receptor (GR) and progesterone receptor (PR) etc., and has four domains: a DNA-binding domain (DBD), a ligand-binding domain (LBD), an N-terminal domain (NTD), and a hinge region which separates the DBD and the LBD [31]. Most of the point mutations of AR occurs at LBD, indicating the significance of the domain in PCa progression with altered AR signaling. Furthermore, the point mutations at the LBDs can result in the loss of specificity of AR to natural agonists, and are often linked with castration-resistance of the PCa. Other domains might also be associated with the genetic alteration of various key regulators and the aberrant AR signaling, leading to the pathogenesis of PCa. The actions of AR differs based on different activation types of AR, and are related to the activation of multiple signaling cascades. Apart from point mutations of the AR domain, AR amplification is also a frequent issue in CRPC. The overexpression of AR hypersensitizes PCa cells to low levels of androgen, switching the agonists to antagonists, and therefore result in resistance to various AR targeting agents. Moreover, by interfering with AR, some AR co-regulators are also critical in the modulation of gene expression [31]. More than 170 co-regulators have been confirmed to be related to CRPC. For instance, members of the steroid receptor coactivator family (SRC) interact with AR, and are associated with tumor cell proliferation, metastasis, and the activation of tumor promoting cascades like PI3K and AKT/mTOR [31, 32].

Apart from the above mentioned factors, other regulators might also participate in the key activities of the PCa progression and could be targets of multiple therapeutic approaches.

2.4 In vitro models for the preclinical studies of PCa

Multiple preclinical models systems and techniques have been adapted to the study of the complex pathological processes of PCa, and the development of novel cancer precision strategies. Cell lines, patient-derived xenografts (PDXs) and patient-derived organoid/ spheroid models are widely used in PCa related preclinical studies, depending on their advantages and limitations [33].

Three cell lines, LNCaP, DU-145 and PC3 are standard cell models in most of the published in vitro studies. Some new cell lines and new sublines were also adapted for research proposes via genetic alterations, chemical mutagenesis and viral transformation [27, 33]. Established in 1977, the LNCaP cell line was isolated from the metastatic lesion of the left supraclavicular

lymph node of a 50-year-old Caucasian diagnosed with PCa. LNCaP cells are sensitive to androgen and estrogen, and present PSA. The cell line has the lowest metastasis level comparing to the other two [33, 34]. DU145 cells present AR, but are hormone-insensitive and do not present PSA. This cell line with epithelial morphology was derived from the CNS metastasis of a 69-year old Caucasian patient with PCa [33, 35]. The PC3 cell line, with the highest metastasis character among the three, was initiated from the bone metastasis of a 62-year-old Caucasian with PCa in 1979. Similar to DU145 cells, PC3 cells present AR, are androgen-insensitive and do not present PSA [33, 36]. Under laboratory conditions, all of the mentioned cell lines perform adherent or semi-adherent characteristics [33, 34, 36]. The infinity growth, simple application and the high through-put ability of PCa monolayer cell culture has made them perfect in vitro models for the study of PCa tumorigenesis and pharmacological mechanisms, despite some limitations including lack of heterogeneity comparing to in vivo models, and no microenvironment and immune influence [33].

PDXs models are advanced models overcoming some of the limitations of PCa cell lines [33, 37]. The aim of PDXs models is to provide an environment allowing the natural growth of tumor cells, normally generated by transplanting cells or tissues derived from primary or metastasis lesions of a patient into immunodeficient mice. Benefited from the progress of tissue engineering technique, PDXs show advantages in retaining cellular heterogeneity and molecular diversity including mutations of the tumor, and possessing tumor microenvironment [33, 37]. The initial problem of poor transplantation success rate has been improved by current technical innovations including the option of highly immunodeficient mice, and the co-injection of extracellular matrix (ECM) along with PCa tissues. The mouse and human prostates exhibit cellular similarities as well as anatomic differences, thus, the differences of tumor microenvironment between human and mouse remains a problem to discuss [33].

The recently developed three-dimensional organoids or spheroids cultures from patients-derived samples retain the original characteristics of the tumor by allowing physiologically relevant cell-cell or cell-matrix contacts and interactions, exhibiting gene expression and signaling pathway profiles, possessing cellular heterogeneity and structural complexity which reflect in vivo tumorigenesis, and therefore attract substantial attention. The culture systems enable the study of host-tumor interactions and model tumor growth determinants, thus play an increasingly significant role in the cancer target discovery and drug development [33, 38]. However, the lack of tumor microenvironment and the poor success rate especially from primary hormone-naive cancer types remain the biggest problem to conquer [33].

2.5 The history and the modern perspectives of the Traditional Chinese Medicine (TCM)

Traditional Western and Chinese herbal medicine agreed on the concept of using herbs for multiple therapeutic approaches [39].

Chinese herbal medicine has a history of over centuries. The oldest herbal classic in China, *Shen Nong's Herbal Classic* (神农本草经, ***Shénnóng Běn Cǎo Jīng***) which classifies 365 species of roots, grass, woods, into three categories of herbal medicine was written around 206 B.C. to 220 A.D and is believed to be the first book contributed to the description of herbs and their therapeutic values [40]. In 659 A.D, the first pharmacopoeia, *Tang Materia Medica* (唐本草 also known as *Xin Xiu Ben Cao* 新修本草) was published by the government of Tang Dynasty (618 – 907 A.D.). Documenting a total of 850 drugs, it is widely accepted as the first pharmacopoeia with legal effect and the first medicinal book published by the organ of power. Completed in 1578 and printed in 1596, the *Compendium of Materia Medica* (*Ben Cao Gang Mu* 本草纲目) provided not only information on the classification, compilation and formation of the traditional medicine, but also other related information including pharmaceutics, chemistry, biology, geography and geology. These ancient classics have largely contributed to the evolution of traditional and folk medicine [40, 41].

The development of modern chemical and analytical techniques has enabled the application of traditional medicinal herbs and their chemical compounds in numerous molecular research. Combined with modern biochemical methods, traditional Chinese medicinal herbs have been proved to exhibit multiple therapeutic effects, including anti-tumor, anti-oxidant, immune stimulatory, anti-inflammatory, analgesic, and regulation of digestive systems etc., and become candidates of first line, complementary and alternative medicine [2, 42, 43, 44].

Artemisinin, for instance, is an example of modern application of the bioactive compound from a traditional Chinese medicinal herb. The Nobel Prize winning drug is extracted from *Artemisia annua* (Qing Hao) from the *Artemisia* family, which has been prescribed in traditional Chinese herbal practice for thousands of years. Nowadays, Artemisinin-based combination treatment (ACTs) is globally the standard treatment for malaria induced by all kinds of *Plasmodium* [42, 45]. In spite of this, other Chinese medicinal herbs like *Panax quinquefolius* saponins (PQS) and *Coptis chinensis* have been proved to have beneficial properties including anti-cancer activity and anti-inflammatory effects [2, 46].

2.6 *Curcuma longa* and its bioactive compounds

Curcuma longa (Jiang Huang in Chinese) is a flowering plant which belongs to the family Zingiberacere. In China, it has been first documented as herbal medicine in 659 AD and has been widely applied to medical practice since then [41]. The most commonly used part of the plant is the dried rhizome, *Curcumae longae 19cetoni*, which can be made into dark yellow powder for longer storage. *C. longa* has a long history as herb, spice and colorant in South, Southeast, and East Asian countries and is nowadays becoming increasingly popular in Western countries [12, 47].

C. longa has been demonstrated to have no toxicity [30]. The herb along with its three main compounds, curcumin, demethoxycurcumin, and bisdemethoxycurcumin (Table 1), have been proved to present pleiotropic pharmacological effects, including anti-inflammatory, antioxidant, antimicrobial and anticancer effects by numerous studies [43]. The therapeutic property of *C. longa* and its bioactive compounds against different types of cancer by modulating multiple molecular regulators and interfering with various signaling pathways has attracted common attention [48, 49, 50, 51].

Table 1. Main compounds of *C. longa* [52].

Compound	**Chemical structure**
Curcumin	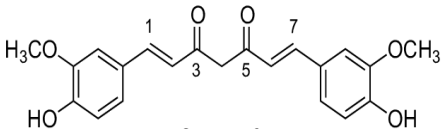
Demethoxycurcumin	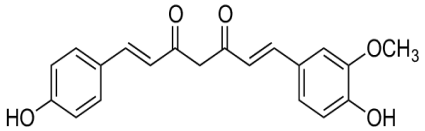
Bisdemethoxycurcumin	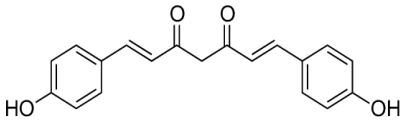

In order to have a brief view of the possible therapeutic targets and mechanism of *C. longa* on Pca based on the existing evidence and knowledge, we performed a Network Pharmacology Analysis in cooperation with the China Academy of Chinese Medical Sciences (Fig. 1). The three main compounds of *C. longa*, marked as JH1, JH2 and JH3 were established using the Traditional Chinese Medicine Systems Pharmacology Database and Analysis Platform

(TCMSP) and the gene targets were set up via the Swiss Target Prediction Database [53]. The outcome suggested that, curcumin (JH1) is associated with the most of the Pca-related genes, including a bunch of oncogenes and tumor-suppressors of multiple cancer types, as well as some Pca-specific genes. Demethoxycurcumin (JH2) is closely related to genes such as the progesterone receptor gene (PGR), a crucial player in the development of androgen independent state of Pca; the gamma catalytic subunit of phosphatidylinositol-4,5-bisphosphate 3-kinase (PIK3CG), a potential therapeutic target for mCRPC patients; and nuclear receptor coactivator (NCOA2), a significant candidate in the treatment of aggressive Pca [54, 55, 56]. Bisdemethoxycurcumin shows correlation with PGR, NCOA2 and a tumor suppressor gene NR3C2 [57].

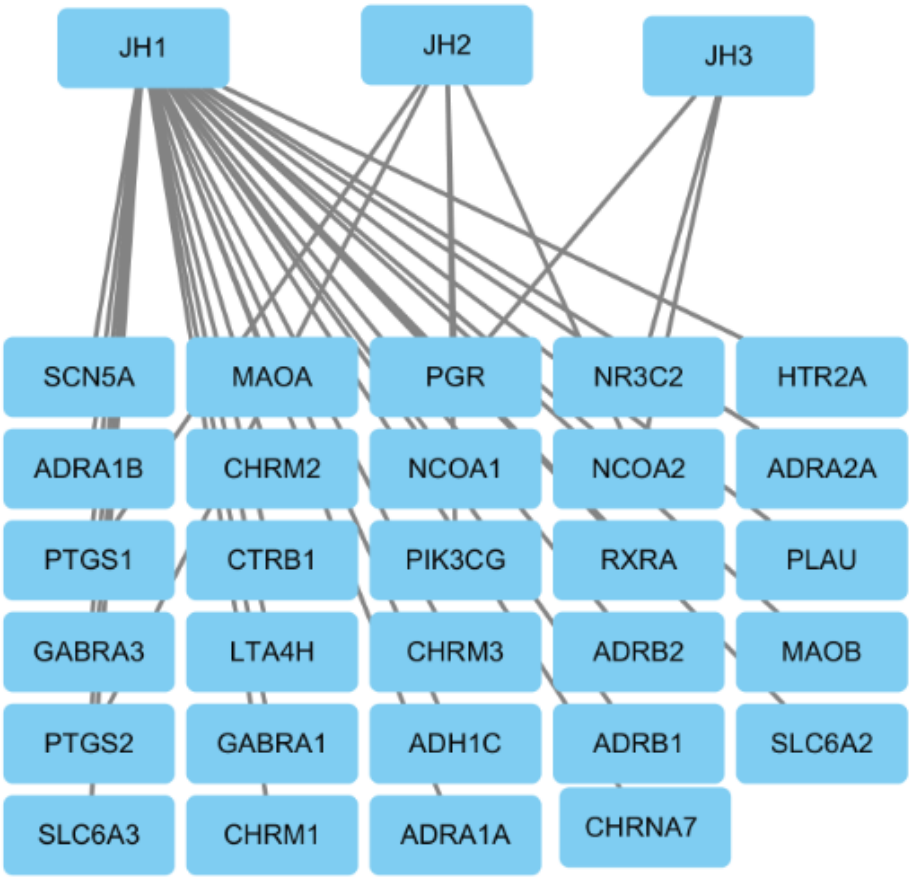

Figure 1. Network Pharmacology Analysis of *C. longa* compounds

A further investigation on the potential signaling pathway using the KEGG Pathway Enrichment Analysis was performed (Fig. 2). The outcome indicates significant enrichment of cancer-related pathways including non-small and small cell lung cancer pathways, cGMP-PKG

signaling pathway, calcium signaling pathway etc. The multifunctional cGMP-PKG pathway was reported to be an endogenous apoptotic signaling cascade in various types of cancer, while calcium signaling pathway is crucially associated with the progression of different types of cancer [58, 59].

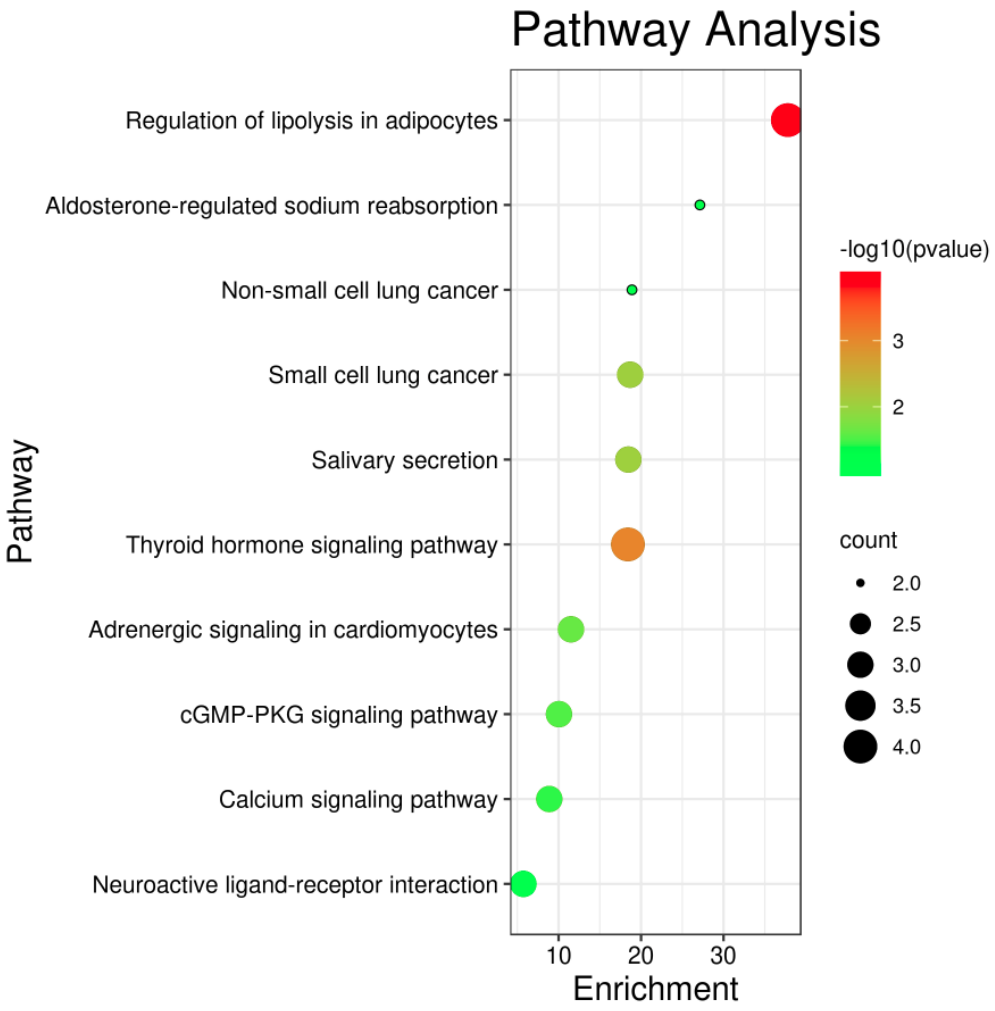

Figure 2. KEGG Pathway Enrichment Analysis.

Previous research already demonstrated the anti-tumor property of *C. longa* on different types of cancer, including Pca [43, 48, 49].

The potential of *C. longa* in suppressing tumor invasion, by down-regulating cell cycle genes and tumor suppressor genes p57kip2 and Rad9 in PC3 prostate cancer cell line has been

confirmed in a study using Ethyl Acetate Fraction of *Curcumae longae Rhizoma* with concentrations between 2 to 6 µg/ml [49].

However, existed studies using *C. longa* are crucially limited. In various studies, curcumin, the main compound of *C. longa* has presented cytotoxic effect on PC3, LNCaP and DU145 Pca cell lines by inhibiting cell proliferation and inducing apoptosis [50, 60, 61].

Protein kinase B (PKB/Akt), encoded by the protooncogene cAkt, plays a role in stimulating cell proliferation as well as inhibiting apoptosis, and is, therefore, a significant cell survival factor. According to an in vitro study, after treating three kinds of Pca cell lines, LNCaP, PC3, and DU145 with 35 µL, 35 µL, and 14 µL curcumin, the activation of Akt has been strongly inhibited, detected by specific antibodies. In this way, curcumin might show its anticancer activity by altering the cell survival factor PKB [60].

Inhibitor of DNA binding 1 (Id1) is a transcriptional factor that belongs to the family helix-loop-helix (HLH). It functions as a promotor that participates in several significant cellular steps and is closely related to apoptosis, cell proliferation, migration, and angiogenesis in Pca cells. According to the group of Yu *et al.*, curcumin down-regulates the mRNA and protein levels of Id1 both in vitro and in vivo. In the in vitro study, a maximum concentration of 20 µm was added to PC3 cell lines for 48h while in the in vivo study, curcumin concentration of 100 mg/kg in 0.1 ml medium was injected into mice models weighted between 15-18 g [50].

The production of intratumoral androgen, such as testosterone and dihydrotestosterone biosynthesis, plays a role in the pathogenesis of castration-resistant Pca. It has been demonstrated that curcumin leads to a decrease in the biosynthesis of testosterone and dihydrotestosterone by up-regulating the expression of Aldo-Keto reductase 1C2 (AKR1C2). The 3-ketosteroid reductase down-regulates dihydrotestosterone level and inhibits the activation of the AR, at the same time alters the expression of different enzymes related to testosterone production in Pca cell line LNCaP. Furthermore, the in vivo study using the transgenic adenocarcinoma mouse prostate (TRAMP) model presents similar result in the increase of testosterone and dihydrotestosterone biosynthesis [61].

The group of Choi *et al.* found that curcumin suppresses the expression of AR in a dose-dependent manner (from 0 to 30 um), by regulating the intracellular level of β-catenin, one of the coregulators that interacts with AR and modulates its transcriptional activity, in LNCaP cell line. In the in vitro study, curcumin suppresses the phosphorylation of GSK-3β, which determines the intracellular level of β-catenin, and therefore interferes with the Wnt/ β-catenin pathway, which has been proved to have a crucial role in the pathogenesis of Pca [62].

Another study from the year 2018 has confirmed the essential role of curcumin in JNK pathway, which was considered as one of the main signaling pathways in different tumor pathogenesis.

In this study, curcumin inhibits the growth of Pca in vivo and suppresses JNK pathway epigenetically by decreasing the phosphorylation level of JNK as well as the level of H3K4me3, an epigenetic marker associated with tumor progression, in LNCaP cell lines [48, 63].

Moreover, curcumin has been proved to have promising effects in other oncogenic processes including cell cycle arrest, cancer invasiveness and metastasis [64, 65, 66].

3 Aims and objectives of the study

3.1 Aims

The aims of this study are to evaluate the anti-cancer activity of the Chinese medicinal herb *Curcuma longa* in human prostate cancer cells, to understand the mechanisms involved, and to discover potential biomarkers for the early diagnosis and treatment of prostate cancer.

3.2 Objectives

- To perform the quality control assessments of the purified *C. longa* extract.
- To evaluate the cell viability of different Pca cell lines after treatment with *C. longa*.
- To determine the amount of apoptotic and necrotic cells after treatment with *C. longa*, using the Annexin and propidium iodic (PI) staining.
- To study the expression level of three cancer-related genes and their corresponding proteins by RT-qPCR and Western blot.
- To explore the gene expression profile of the anti-cancer effect of *C. longa* by RNA sequencing.
- To investigate the interactions among multiple sets of genes and perform pathway analyses.

4 Methods

4.1 *C. longa* sample preparation

The purified *C. longa* extract was supported by St. Anna-Apotheke, Firma Magister Martin Diskar pharm. Produkte e.U., Vienna, Austria. The *C. longa* powder was dissolved in RPMI-1640 culture medium (1%Pen/Strep, 10% FBS, 1% glutamine, and 1% Hepes, GIBCO, Dublin Ireland) for cell culture experiments. The samples were heated at 60°C for 30min for getting better solubility. After the heating process, no precipitation was visible by naked eves and under the light microscope (10X, 40X), and the *C. longa* samples exhibited uniform dark

yellow color. The stock samples were sterilized using the 0.2 µm Pore PES Membrane Sterile Filters (Corning Life Science, New York, USA).

4.2 Sample stability test

C. longa sample solutions were fresh prepared in two concentrations of 100 µg/mL and 600 µg/mL. The stability of samples at different temperatures (at room temperature, heated for 5 min at 60°C and at 95°C) and pH values were evaluated by measuring OD absorbance of 260 nm and 280 nm using the DeNovix DS-11 Spectrophotometer/Fluorometer Series. The pH value was measured using a pH-meter (827 pH lab, Metrohm, Switzerland) at room temperature. At the first two weeks, samples were measured every day. From day 15, the samples were measured every two days, and from day 31, the samples were measured every week. All the samples for the tests under different conditions were prepared in triplicates.

4.3 Quality control of *C. longa* by High Performance Liquid Chromatography (HPLC)

Using Agilent 1260 Infinity II, we performed a High Performance Liquid Chromatography (HPLC) for the quality control assessments of the purified *C. longa* extract. 1 mg standard sample of curcumin was precision weighed using MT5 0.001 mg Analytical Microbalance (Mettler Toledo, Switzerland) and ultrasonicated for 10 min at 400 W with 1 mL methanol using a KQ-500DE numerical control ultrasonic cleaner (Kunshan, China) for a stock solution of 1 mg/mL. The standard solution was then diluted into 50 µg/mL, and centrifuged at 13000 rpm for 10 min (SL4F Centrifuge, Thermo Fisher Scientific, MA, USA). 0.2 g *C. longa* extract was precision weighted via AT201 0.01 mg Analytical Balance (Mettler Toledo, Switzerland) and ultrasonicated for 15 min at 400 W with 1 mL methanol. After centrifuging for 10 min at 13000 rpm, the supernatant of the sample was collected and diluted to 5 mg/ mL. The sample was then centrifuged again. The supernatant was stored for lateruse. Six samples were prepared following the same procedure. The chromatographic separation was conducted by an Alltima C 18 (250 mm x 4.6 mm, 5µm) liquid chromatographic column. The mobile phases consisted of 24cetonitrile – 4% glacial acetic acid (48:52) with gradient elution. The temperature for the column was 25 °C and the detection wavelength was 430 nm. The injection volumes for the curcumin standard solution and the *C. longa* extract samples were 5 µL, with a flow rate of 1 mL/ min. Each sample was injected three times. The accurate mass and elemental composition was analyzed by the MassLynx V4.1 software (Waters Co., Milford, MA, USA).

4.4 Cell lines and cell culture

Human prostate cancer cell lines PC3, DU145, and prostate epithelial cell line PNT2 were used in this study. We incubated the cells in RMPI-1640 medium at 37°C with 5% CO_2, in a 25 cm^2 Nunclon tissue culture flask (Thermo Scientific, Waltham, MA, USA). The cells were supplied with fresh medium every 48 h. After the PBS wash, cells were centrifuged at 900 rpm for 5 min at room temperature. The cells were collected and calculated by a TC20 automated cell counter (BIO-RAD, CA, USA) and split into the tissue culture flasks for further experiments. In different experiments, the cells were treated with different concentrations of *C. longa* (0, 50, 100, 200, 400, and 800 µg/mL).

4.5 Cell imaging

0.3 x 10^6 cells/mL DU145 were seeded in 6-well plates and incubated with increasing concentrations of *C. longa* (0, 50, 100, 200, 400, and 800 µg/mL) for 48 h. After the incubation, cells were imaged using the EVOS® digital inverted microscope (Thermo Fisher Scientific, Germany).

4.6 Cell viability assay

DU145, PC3, and PNT2 cells were seeded in the 96-well plates (Thermo Fisher Scientific, MA, USA). Following the incubation of 24 h at 37°C, the cells were treated with increasing concentrations of *C. longa* (0, 50, 100, 200, 400, and 800 µg/mL) for 48 h. The cell viability of all three cell lines was measured after the treatment using a CellTiter-Blue Cell Viability Assay Kit (Promega Co., WI, USA). The absorbance was measured using a Tecan microplate reader (Epoch, Bio-Tek Instruments, Winooski, VT, USA) at 560 nmEx/ 590 nmEm. We calculated the data as a ratio of treated versus untreated cells (vehicle set at 100%).

4.7 Apoptosis detection

To detect the apoptosis of DU145 cells after 48 h of *C. longa* treatment, we applied a FITC Annexin V Apoptosis Detection Kit with PI (Biolegend, CA, USA). DU145 cells were treated with 400 µg/mL and 800 µg/mL of *C. longa* for 24h at a seeding density of 10^5 cells/ mL in 6-well plates. Cells treated with PBS were set as negative control respectively. After 24

h of incubation, cells were harvested, washed twice with PBS, and centrifuged. Afterwards, cells were resuspended in 300 µL binding buffer. 10 µL Annexin V-FITC and 5 µL propidium iodide (PI) were added to the cell suspension and incubated for 15 min without exposure to light at room temperature. After incubation, 400 µL binding buffer was added. The flow cytometer (BD FACS Canto™II, BD Biosciences, CA, USA) was used to analyze the stained cells under the excitation wavelength of 488 nm. We repeated the experiment three times, to obtain mean value. The data was analyzed with the help of FlowJo software V10.

4.8 Quantitative detection of mRNA expression via qRT-PCR

DU145 cells were incubated with increasing concentrations of *C. longa* (0, 50, 100, 200, 400, and 800 µg/mL) for 48 h. The total RNA of DU145 was isolated following the TRIzol Reagent protocol (Thermo Fisher Scientific, MA, USA). After seeding 0.7 x 10^6 cells / well in 6-well plates and incubating them for 48 h, cells were harvested using TRIzol reagent. 200 µL chloroform was then added to the harvested samples in TRIzol reagent. The mixture was separated into a lowered phenol chloroform, an interphase, and a transparent upper aqueous phase after centrifuged for 15 min at 12000 g at 4°C. The upper phase was collected into the new tubes. 500 µL isopropanol was added to the samples to ensure the stability of the RNA. After 10 min of centrifugation at 12000 g, 4°C, the total RNA precipitate formed a white pellet at the bottom of the tube. The supernatant was removed and the pellet was washed twice with 900 µL 75% ethanol. During the washing step, the pellet was resuspended in ethanol and centrifuged for 5 min at 7500 g, 4°C. The ethanol supernatant was removed and the RNA pellet was left air dry for 15 min until no liquid can be observed. At last, the pellet was dissolved in 20–50 µL Rnase-free water for downstream application or storage at -80°C. The concentrations of the isolated RNA samples of DU145 cells were quantified using the DeNovix DS-11 Spectrophotometer/Fluorometer Series, before synthesized into cDNA strands via OneScript cDNA Synthesis Kit (Applied Biological Materials Inc. (abm), Richmond, Canada). The fold changes of the following cancer related genes (p21, TMEM79, and ACOXL) were determined after *C. longa* treatment with the help of qRT-PCR. 18S served as a control.

For qRT-PCR analysis, we prepared the reaction mixture containing 10 pmol/µL of SYBR Green Master Mix (Applied Biosystem, USA). The respective forward and reverse primers were generated using the NCBI BLAST and listed in Table 2.

Table 2. The sequences for the human-specific primers p21, TMEM79, ACOXL and 18S.

primer	forward	reverse
p21	AGTCAGTTCCTTGTGGAGCC	CATTAGCGCATCACAGTCGC
TMEM79	GTCTTTCCGGCTTCTCCAAA	GTGGGTACACTGTCCGTTCTC
ACOXL	GGAGCCTCAAGAACGAGCTG	AGAGGTCAAAGGTGGCTTCG
18S	CTCAACACGGGAAACCTCAC	CGCTCCACCAACTAAGAACG

The program for thermal cycling conditions was: 10 min at 95°C, followed by 40 cycles for 15 s at 95°C, 1 min at 60°C, and 15 s at 95°C. During the amplification, an incremental temperature increases from 60°C to 95°C. Afterwards, a melting curve analysis of the products was performed. The qRT-PCR was performed on QuantStudio™ 5 Smart Start Real-Time PCR System (Thermo Fisher Scientific, MA, USA) and analyzed on the corresponding software. The experiments of all the genes were repeated three times in duplicate. Relative expression levels of the genes were assessed using the 2-ΔΔct method.

4.9 Western blot analysis

DU145 cells were centrifuged and collected after 48 h of treatment with *C. longa* with increasing concentrations (0, 50, 100, 200, 400, and 800 µg/mL), and lysed following the RIPA Lysis and Extraction Buffer manual from Thermo Fisher Scientific. RIPA buffer was enriched with a Pierce™ Protease Inhibitor Tablet (Thermo Scientific, USA) to avoid protein degradation. After centrifugation, the supernatant of the samples was collected. The collected supernatant samples were then diluted to an appropriate concentration, mixed with Laemmli Buffer, and denatured at 95°C for 5 min. for SDS-PAGE, the samples were loaded on 4-15% Mini PROTEAN TGX gels (Bio-Rad, Hercules, CA, USA). The proteins were separated according to their sizes by electrophoresis for 1 h at 100 V. Subsequently, the proteins were transferred to a polyvinylidene fluoride or polyvinylidene difluoride (PVDF) membrane (Bio-Rad, Hercules, CA, USA) and blocked in tris-buffered saline, 0.1% Tween (TBST) buffer with 5% nonfat milk. Blots were incubated with 1:2500 dilution for p21 antibody; 1: 1000 dilution for TMEM79 antibody; 1: 500 dilution for ACOXL antibody and 1:1000 dilution for β-actin antibody overnight at 4°C, followed by incubations of 2 h with 1: 4000 dilution of goat anti-rabbit IgG (H + L)

secondary antibodies. The protein bands were stained using Amersham™ ECL™ Prime Western Blotting Detection Reagent (GE Healthcare, UK), and visualized under ChemiDoc™ Imaging System (Bio-Rad, CA, USA). β-actin was used as a control protein.

4.10 Illumina RNA sequencing

RNA samples were isolated following the same steps as described in chapter 8. The isolated, quantity determined and quality controlled total RNAs were 28ubmitted to the Core Facilities Genomics of the Medical University of Vienna for RNA sequencing. Sequencing libraries from the total RNA samples were prepared using the QuantSeq FWD protocol (Lexogen). Optimal numbers of PCR cycles were determined by qPCR following the library prep manual. Libraries were QC-checked on a Bioanalyzer 2100 (Agilent) via a High Sensitivity DNA Kit for correcting the insert size and then quantified using Qubit dsDNA HS Assay (Invitrogen). The pooled libraries were sequenced on a NextSeq500 instrument (Illumina) in 1x75bp single-end sequencing mode. Around 7 million reads were performed per sample. Reads in fastq format using the Illumina bcl2fastq command line tool (v2.19.1.403) were generated. Reads were filtered using cutadapt version 1.15 to remove reads with N's and trim polyA tails. Reads in fastq format were aligned to the human reference genome version GRCh38 with Gencode 29 annotations using STAR aligner version 2.6.1a in 2-pass mode. STAR was used to count the raw reads per gene. Differential gene expression was calculated using DESeq2 version 1.22.2 [67, 68, 69, 70, 71].

4.11 Statistical analysis

All the data are expressed as mean ± SEM/SD of three independent experiments and three technical copies. One-way ANOVA analysis was calculated using the GraphPad Prism 9 software. Statistically significant results among means were set at *$p < 0.05$, **$p < 0.01$, ***$p < 0.001$.

The cell viability assay data was calculated as a ratio of treated versus non-treated cells, with the vehicle set as 100%.

The data of the apoptosis detection was analyzed with the help of FloJo software V10.

The obtained Illumina RNA sequencing data consists of three parts of different analyses: gene expression analysis, gene ontology (GO) analysis and pathway analysis.

4.12 Bioinformatic analyses of the gene profiles and the signaling pathways

The differential gene expression data from the Illumina sequencing of the 12 h and the 24 h treated samples comparing to the untreated samples, were selected with an up-/downstream of more than two-fold in the *C. longa* treated DU145 cells compared to the non-treated cells. We listed the most cancer-related and Pca-specific genes with top regulation scores (Log2 fold change) and $p < 0.05$, and created a heat map using GraphPad Prism 9 software.

Additionally, a volcano plot using VolcaNoseR (https://huygens.science.uva.nl/VolcaNoseR/) to visualize the expression changes of the samples after 24 h of *C. longa* treatment, based on the distance to the origin was created [72]. log2FoldChange was selected for X-axis, and minus_log10_padj was set as Y-axis. A fold change threshold between -1.1 and 1.1, and a significance threshold < 1.5 was selected, Mahattan distance was used as the criterion for ranking hits.

A Gene Set Enrichment Analysis (GSEA) comparing the data of untreated DU145 cells with 24h treated DU145 cells, using fifty cancer-related hallmark gene sets from the Molecular Signatures Database (MsigDB) v7.5.1 was conducted using BubbleGUM (GSEA Unlimited Map) software “Signal to Noise” settings [73, 74, 75, 76]. The affected regulators were plotted in the volcano plot using GraphPad Prism 9 software.

For the analyses of the affected signaling pathway, the gene ontology (GO) functional annotation was analyzed based on the DAVID Bioinformatic Resources (2021 update) (https://david.ncifcrf.gov/tools.jsp) [77, 78]. The analyses was based on the background of the Homo sapiens species, GOTERM_BP_DIRECT, GOTERM_CC_DIRECT, and GOTERM_MF_DIRECT were selected among the Gene_Ontology database, and 497 DAVID IDs were detected. The dysregulated pathways of biological process (BP), cellular component (CC), and molecular function (MF) were ranked based on the altered gene counts.

Subsequently, a Pathway over-representation analysis using Ingenuity Pathway Analysis (IPA) using the QIAGEN IPA (QIAGEN Inc. version 01-12, https://digitalinsights.qiagen.com/IPA) was performed [79]. Genes were prefiltered to remove the genes with low expression levels. Top 20 dysregulated pathways with the highest –log (p-value) were listed.

5 Results

5.1 *C. longa* is temperature and pH stable in solutions

In order to evaluate the stability of *C. longa* in different experimental concentrations over a longer period of time, the stability of different temperatures and pH velums were measured. We used two concentrations of *C. longa* (100 µg/mL and 600 µg/mL) for the experiments. Samples were prepared at room temperature (RT), heated for 5 min at 60C° and at 95°C for the measurements. The absorbance of the samples under two UV wavelengths (OD 260 and OD 280) was measured (Fig. 3a, b). The pH values of the two concentrations of *C. longa* were measured at room temperature with the same timeline (Fig. 3c). Results indicated that both low and high concentrations of *C. longa* samples remain stable from day 1 to day 59, at all three different temperatures. The pH values of the samples were stable at room temperature.

a

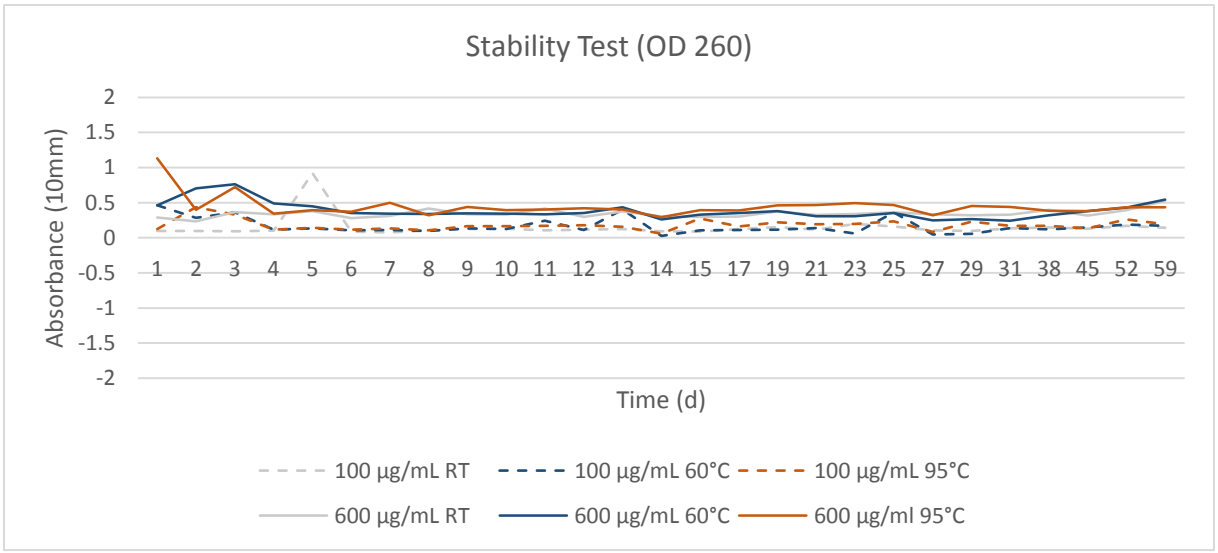

b

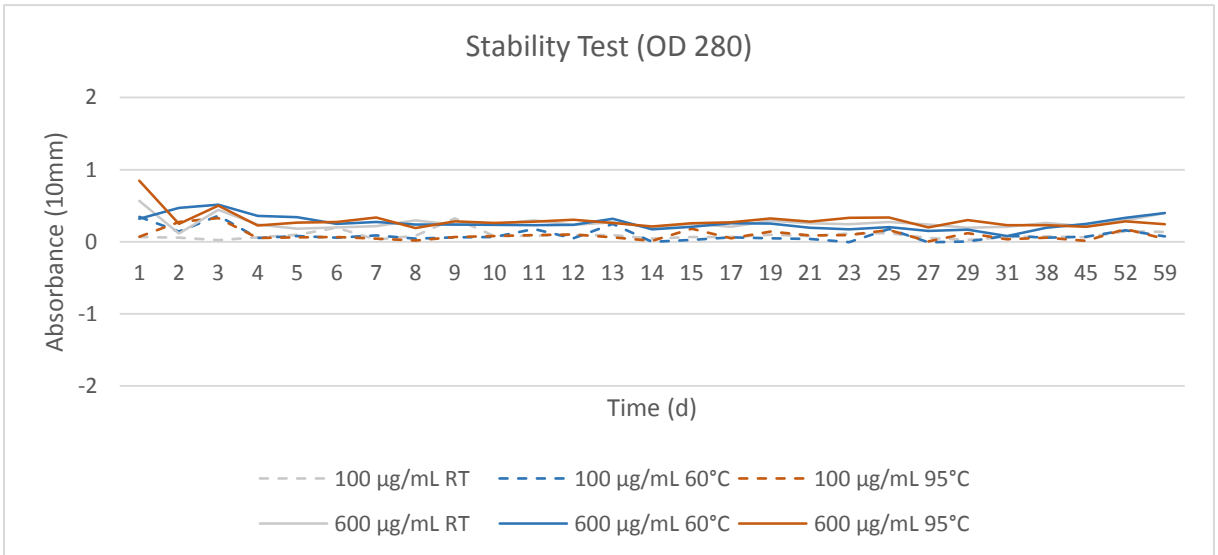

C

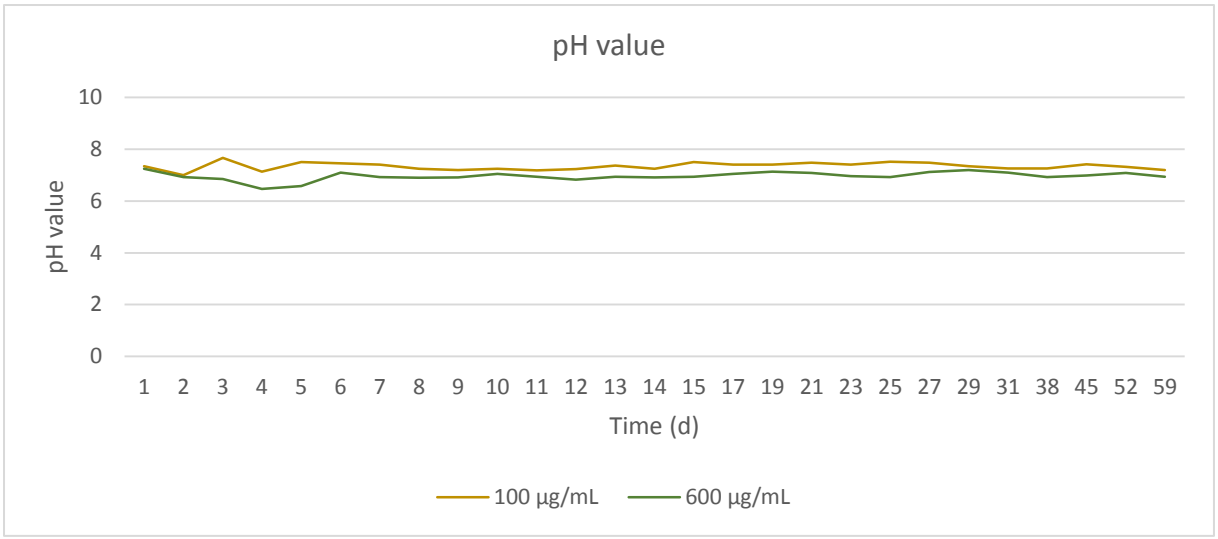

Figure 3. *C. longa* is temperature and pH stable in solutions. *C. longa* remains thermal stable under three different temperatures (a, b). 100 µg/mL and 600 µg/mL *C. longa* were treated at RT, 60°C, and 95°C. The absorbance of each sample was measured using NanoDrop under UV OD 260 and OD 280 from day 1 to day 59. The pH values of *C. longa* remain stable. The pH values of 100 µg/mL and 600 µg/mL *C. longa* were measured using a pH-meter from day 1 to day 59 at RT ©.

5.2 Quality control of *C. longa* by HPLC

We performed HPLC for the quantity measurement and quality control of the bioactive compounds in *C. longa*. *C. longa* was diluted in methanol and prepared into six samples of 5 mg/mL. Three major compounds of *C. longa* were identified by the retention time and the content of the reference compounds. The retention time of the three main peaks were 20.8 min (curcumin), 19.0 min (demethoxycurcumin), and 17.3 min (bisdemethodycurcumin) [52]. The characteristic peaks of the six samples remained consistent and showed similar fingerprints (Fig. 4). The concentration and percentage of the main active compound curcumin were 53.90 µg/mL and 0.106%, calculated using a standard curcumin solution (area under the peak: 1355.537 mm^2, concentration: 51.5 µg/mL), via the following formula:

$Area_{standard}/Area_{sample}=Concentration_{standard}/Concentration_{sample}$

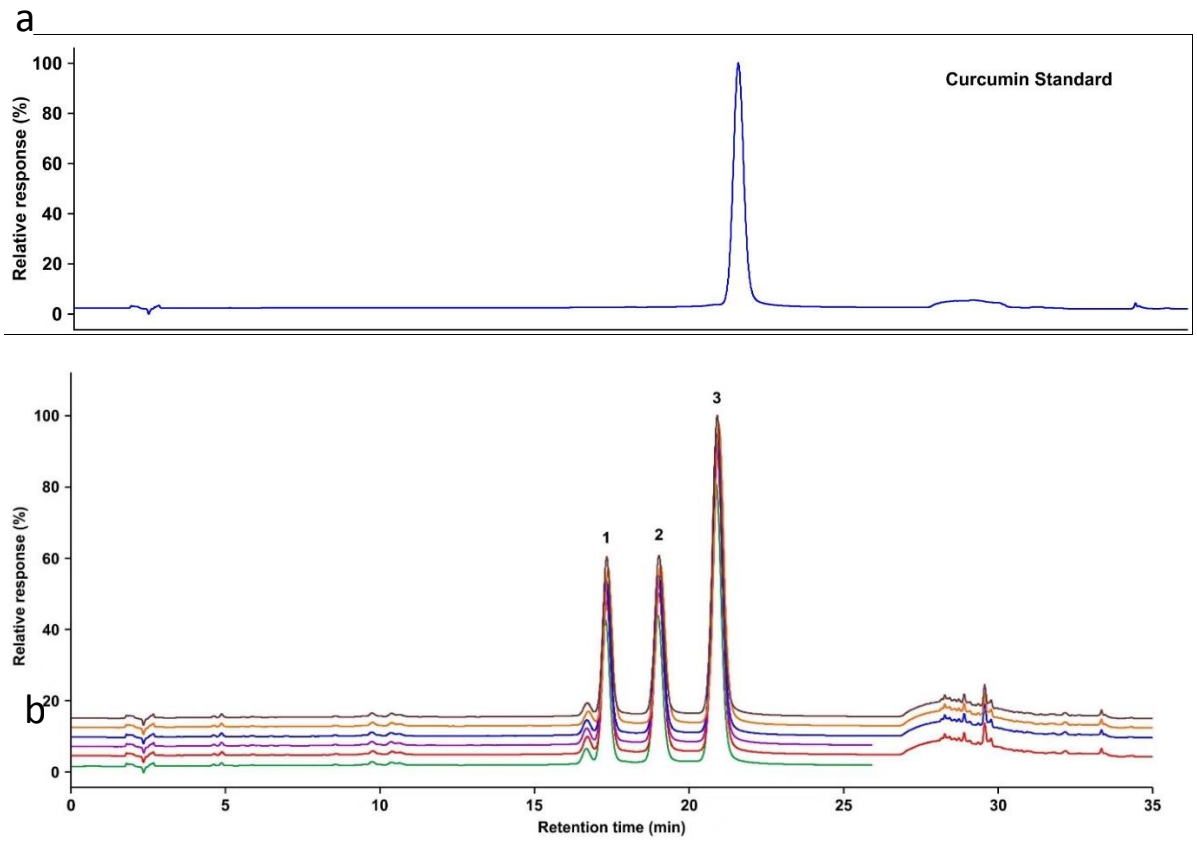

Figure 4. Qualification of *C. longa* by HPLC. The three main characteristic peaks represent bisdemethoxycurcumin (1), demethoxycurcumin (2), and curcumin (3), all six samples showed similar fingerprints.

5.3 *C. longa* inhibited the growth of PCa cell lines DU145 and PC3, and induced cell death

To test the cell growth of Pca cell line DU145 after the treatment with CL at different concentrations, DU145 cells were treated with the following concentrations (0, 100, 200, 400, 600 and 800 µg/mL) of CL for 48h. The microscopic pictures (Fig. 5) show the cell density of the DU145 cells. The cell density decreased with the increase of CL concentration, indicating a dose-dependent inhibition of cell growth after the treatment of CL. At a concentration of 800 µg/mL, the cell density was around 50% compared to the cells at 0 µg/mL.

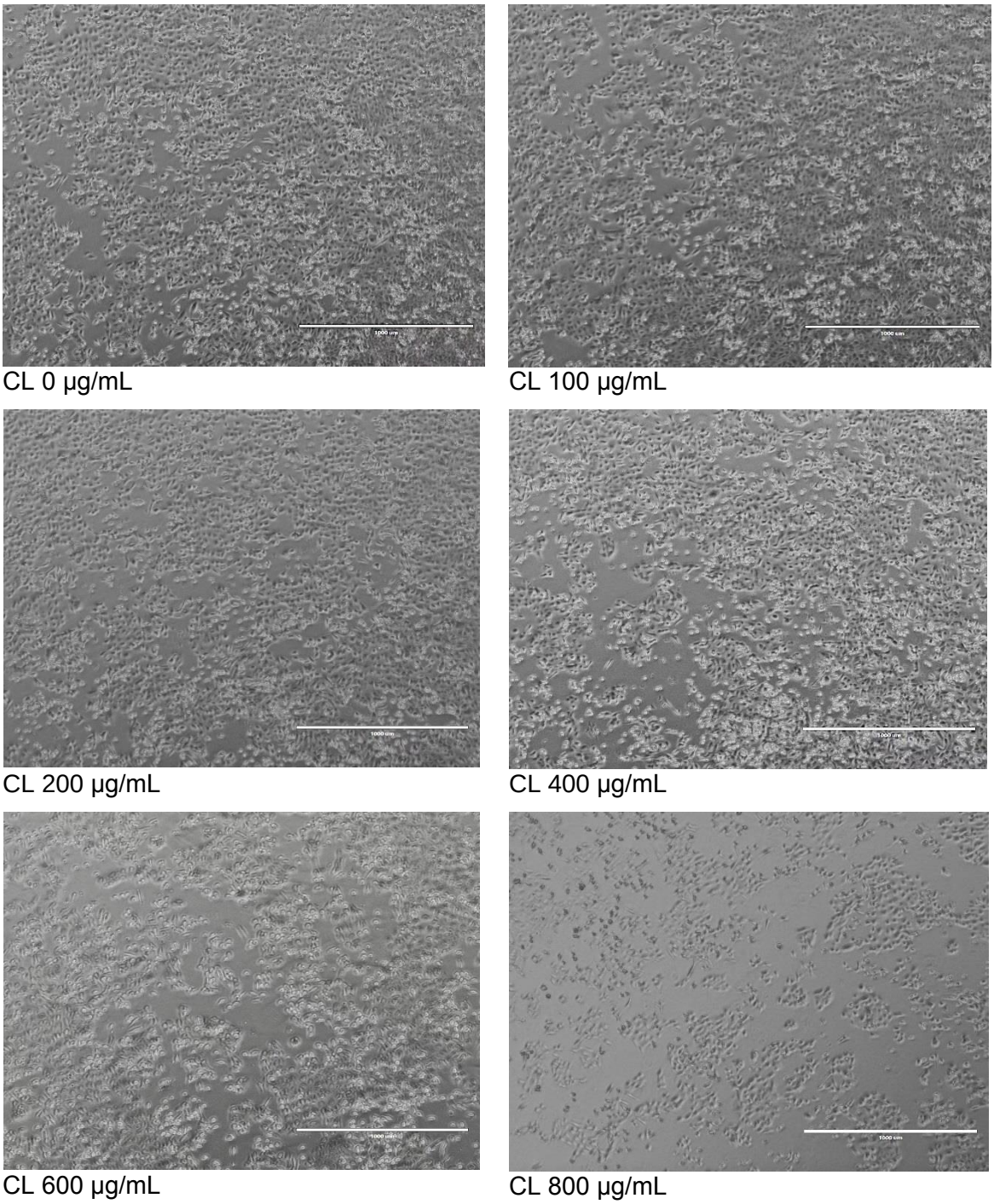

Figure 5. CL inhibited cell growth of DU145 dose-dependently. DU145 cells were treated with increasing concentrations of CL (0, 100, 200, 400, 600 and 800 µg/mL). Cells were photographed using a microscope after 48h treatment.

To determine the cell viability of Pca cell lines DU145 and PC3 after the treatment of CL, cells were treated with the same concentrations of CL (0, 100, 200, 400, 600, and 800 µg/mL) for 48h, and cell viability assay was performed using a Cell Titer-Blue assay kit. The immortalized

prostate epithelial cells PNT2 cells were used as a control group. Dose-dependent decrease of cell viability can be observed in both DU145 and PC3 cells, while PNT2 cells were not affected by the CL treatment. At a concentration of 800 µg/mL, CL induced a reduction of % in DU145 and a reduction of % in PC3 cells, compared to a 0% reduction in PNT2 cells (Fig. 6a, b).

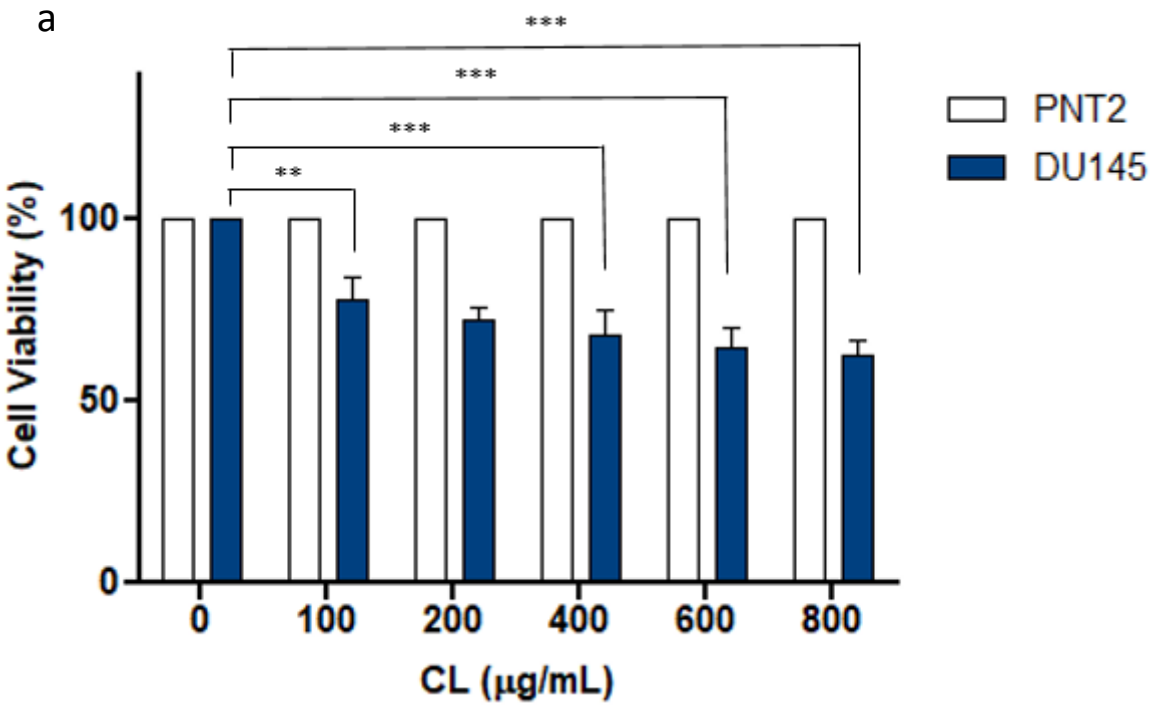

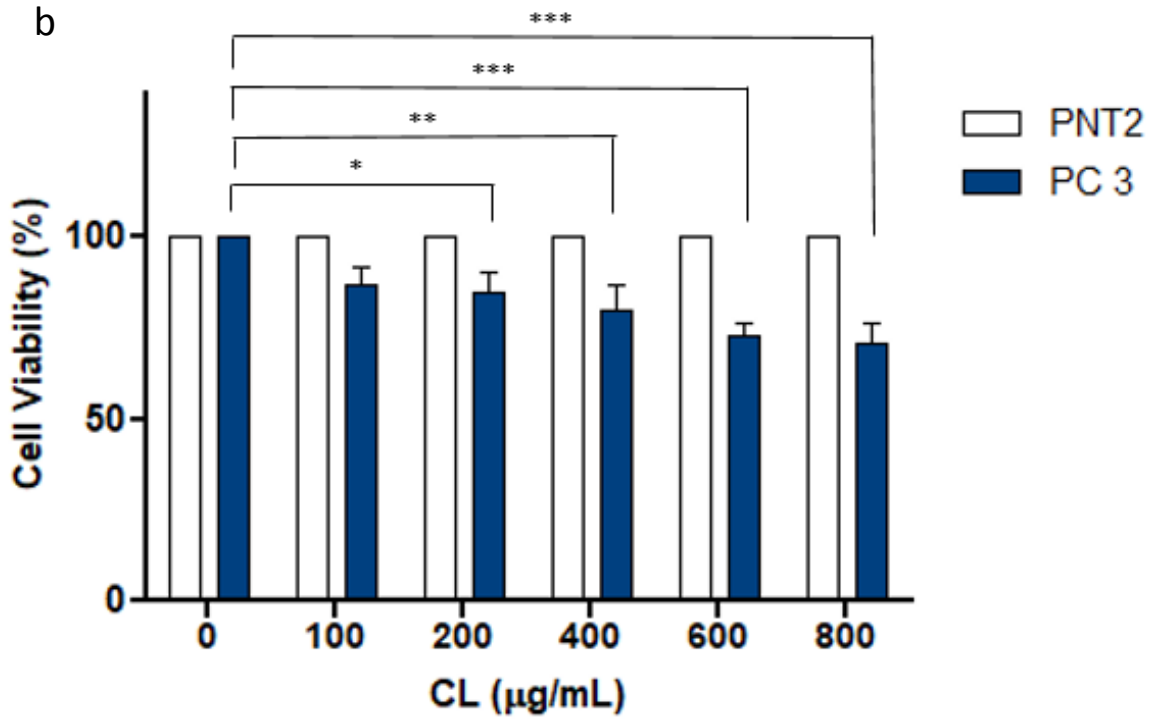

Figure 6. CL induced dose-dependent inhibition in DU145 and PC3 cells. DU145, PC3 and PNT2 cells were treated with increasing concentration of CL (0, 100, 200, 400, 600 and 800 µg/mL) for 48 h. Cell viability (% of control) was measured using a Cell Titer-Blue Assay Kit. Error bars represent standard deviation (SD) from n ≥ 3 independent experiments in triplicate. *, ** and *** represent $p < 0.05$, $p < 0.01$ and $p < 0.001$, as calculated by one-way ANOVA.

We used FITC Annexin V Apoptosis Detection Kit with propidium iodide (PI), to detect the apoptotic and late-apoptotic DU145 cells after the treatment of *C. longa*, and analyzed the samples by a FACS flow cytometer. DU145 cells were treated with a medium and a high concentration (400 µg/mL, 800 µg/mL) of *C. longa* for 24h, cells treated with phosphate-buffered saline (PBS) for 24h were used as control. After the treatment with a medium concentration of *C. longa*, cells presented 2.53% early-stage apoptosis, 61.9% late-stage apoptosis, and 30.8% viability, while cells treated with a high concentration of *C. longa* showed 2.45% early-stage apoptosis, 67.8% late-stage apoptosis and 23.1% viability. Cells incubated in PBS for 24h exhibited 1.33% early-stage apoptosis, 56.5% late-stage apoptosis and 39.1% viability. The percentages of necrotic cells were: 3.01% in PBS incubated cells, 4.74% in cells treated with a medium concentration of *C. longa,* and 6.68% in those treated with a high concentration of *C. longa*. Total apoptosis (early-stage plus late-stage apoptosis) increased from 57.83% in PBS-treated cells to 64.43% and 70.25% in cells treated with medium and high concentration of *C. longa*, which equals a total increase of 11.41% and 21.48%, respectively (Fig. 7).

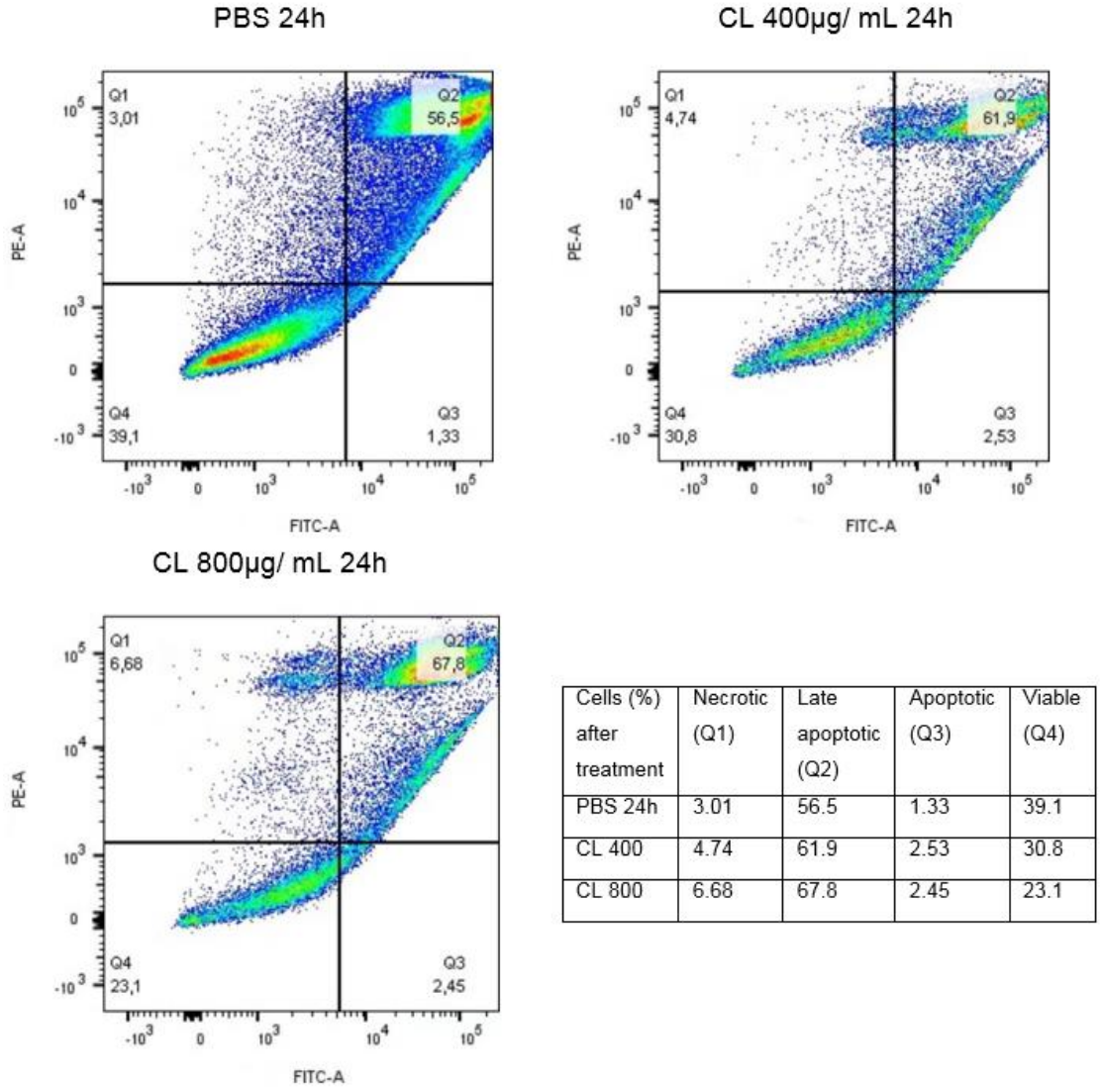

Cells (%) after treatment	Necrotic (Q1)	Late apoptotic (Q2)	Apoptotic (Q3)	Viable (Q4)
PBS 24h	3.01	56.5	1.33	39.1
CL 400	4.74	61.9	2.53	30.8
CL 800	6.68	67.8	2.45	23.1

Figure 7. C. longa induced apoptosis in DU145 cell. DU145 cells were treated with 400 µg/mL and 800 µg/mL *C. longa* for 24h, and incubated with PBS for 24h as a negative control. After the treatment, apoptotic cells were measured with a FITC Annexin V Apoptosis Detection Kit and PI by FACS flow cytometry. Cells treated with a high concentration of *C. longa* (800 µg/mL) exhibited a significant increase in apoptosis, compared to the PBS incubated cells. An increase of 11.41% and 21.48% in total apoptosis were observed in cells treated with 400 µg/mL and 800 µg/mL *C. longa.*

5.4 RNA isolation for qRT-PCR and Illumina RNA sequencing

The total RNA of DU145 was isolated using the TRIzol Reagent. The quantitation of RNA samples with quality assessment was performed and the data was analyzed using Agilent 2100 Bioanalyzer Data/2100 Expert Eukaryote Total RNA Nano Software. The 18S and 28S

peaks are visible at 1,584 [nt] and 3,104 [nt], respectively. RNA area was 174.9, RNA concentration was 71 ng/µl, rRNA Ratio 28S/18S was1.5.

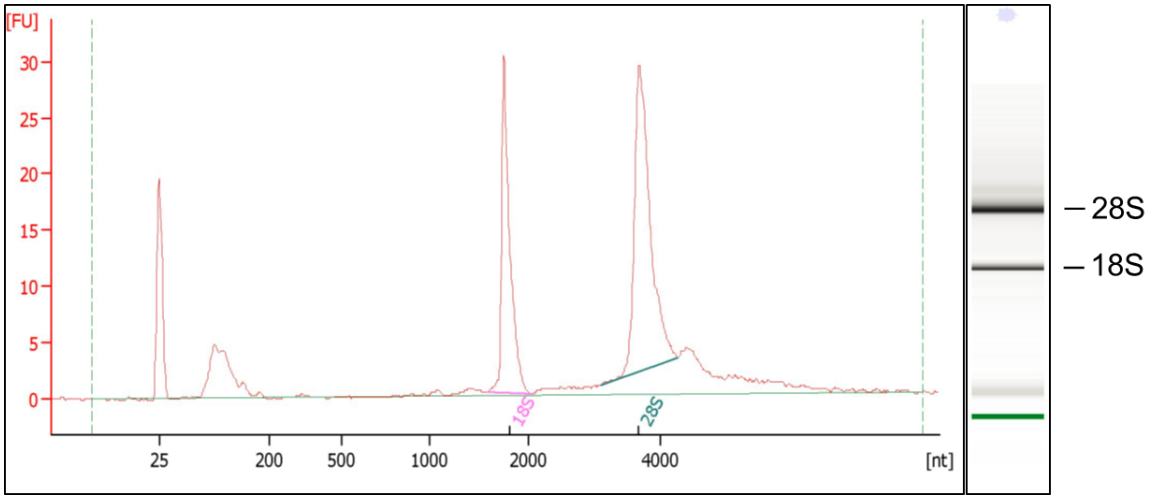

Figure 8. Agilent 2100 Bioanalyzer Data of total RNA sample. The 18S and 28S peaks are visible at 1,584 [nt] and 3,104 [nt], respectively. 2100 Expert Eukaryote Total RNA Nano Software was used for data analysis. RNA area was 174.9, RNA concentration was 71 ng/µl, rRNA Ratio 28S/18S was1.5.

5.5 *C. longa* regulated the gene expression of p21, TMEM79 and ACOXL at the level of RNA and protein

To quantify the expression level of different cancer-related and prostate cancer-specific genes, we performed qRT-PCR and western blot analysis of the gene p21, the transmembrane protein 79 (TMEM79) and the acyl-coenzyme-A oxidase-like protein (ACOXL).

p21 gene, commonly known as a mediator of the tumor suppressor p53, presents anti-cancer activity by inhibiting cell cycle and cell proliferation, which involves multiple pathways dependent and independent of p53 [80]. TMEM79 and ACOXL are two lately published potential biomarkers specific for the diagnosis of PCa, which sensitively and specifically distinguish between benign prostate tumor and Pca [81]. In the qRT-PCR and western blot analysis, the mRNA and protein expression levels of these genes were evaluated, in order to find out whether 48 h *C. longa* treatment alters the expression of these Pca-related gene regulators in DU145 cells. The qRT-PCR results suggested that, 48 h treatment of C. longa significantly up-regulated the gene expression level of p21, TMEM79 and ACOXL in DU145 cells in dose-dependent manner (Fig. 9, *$p < 0.05$, **$p < 0.01$, ***$p < 0.001$). Additionally, the protein bands in the western blot analysis supported the results of qRT-PCR. Upon 48 h *C. longa* treatment, the protein expression levels of p21, TMEM79 and ACOXL increased dose-

dependently in DU145 cells (Fig. 10). Both mRNA and protein expression levels of these genes were consistent.

a

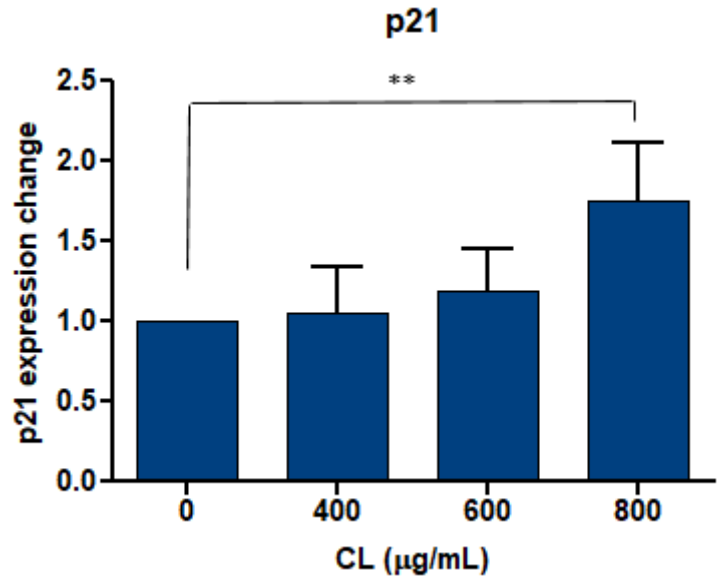
p21
**
p21 expression change
2.5
2.0
1.5
1.0
0.5
0.0
0
400
600
800
CL (μg/mL)

b

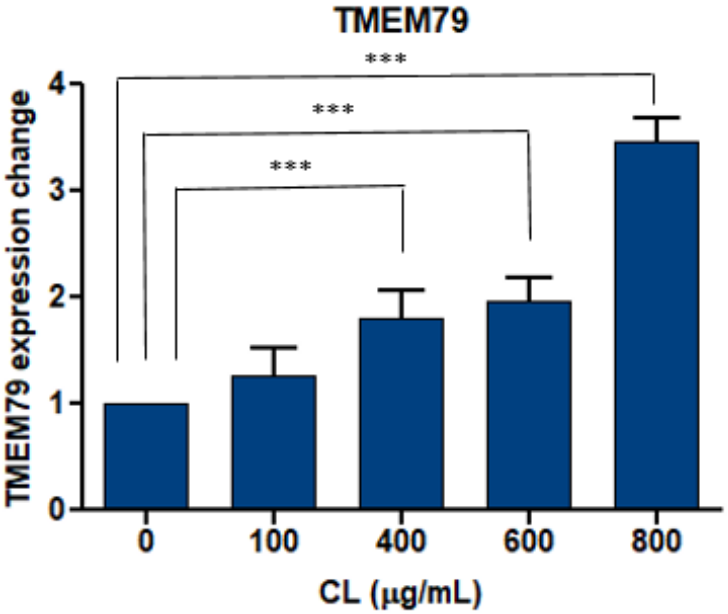
TMEM79
***
***
***
TMEM79 expression change
4
3
2
1
0
0
100
400
600
800
CL (μg/mL)

c

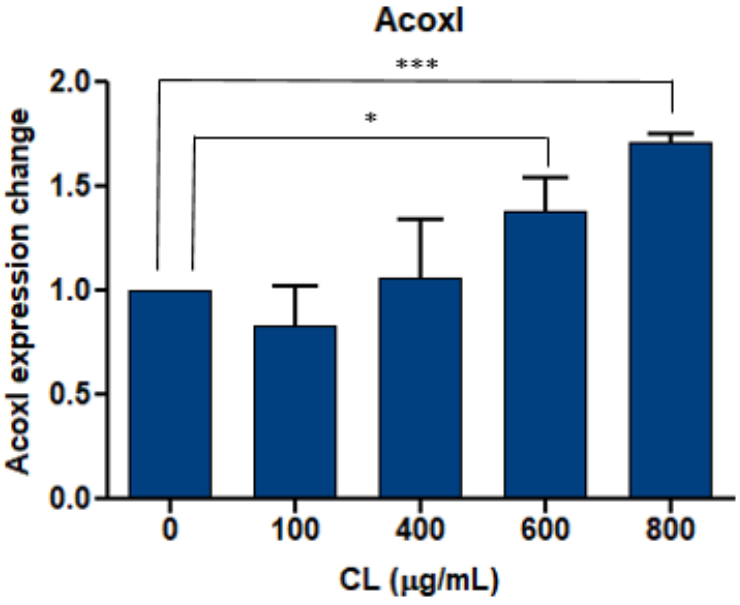
Acoxl
***
*
Acoxl expression change
2.0
1.5
1.0
0.5
0.0
0
100
400
600
800
CL (μg/mL)

Figure 9. *C. longa* regulated the expression of cancer-associated genes at mRNA level. DU145 cells were treated with increasing concentrations (0, 100, 200, 400, 600, and 800 µg/mL) of *C. longa* for 48h. The expression levels of p21, TMEM79, and ACOXL were up-regulated in a dose-dependent manner after the treatment (a-c). The qRT-PCR was performed using a SYBR Green PCR Master Mix Kit. Standard deviations (SD) are represented by error bars from n ≥ 3 independent experiments in triplicate. *, ** and *** represent $p < 0.05$, $p < 0.01$ and $p < 0.001$, as calculated by one-way ANOVA.

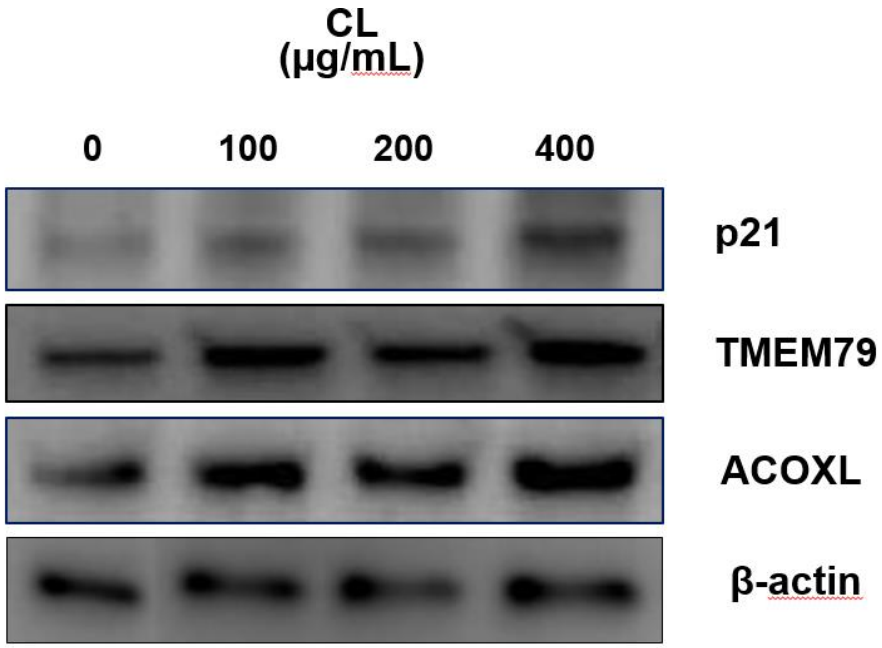

Figure 10. *C. longa* regulated the expression of cancer-associated genes at protein level. DU145 cells were treated with increasing concentrations (0, 100, 200, 400, 600, and 800 µg/mL) of *C. longa* for 48 h. Protein samples were collected for SDS-PAGE and western blotting. β-actin was used as a positive control. The intensity of the protein (p21, TMEM79 and ACOXL) bands increased dose-dependently, indicating dose-dependent up-regulations of the corresponding genes at the protein level.

5.6 *C. longa* regulated the gene expression of various oncogenes and tumor suppressors

To further explore the gene expression profiles in DU145 cells after the treatment of *C. longa*, we performed Illumina RNA sequencing supported by the Core Facilities Genomics of the Medical University of Vienna. DU145 cells were treated with 800 µg/mL *C. longa* for 12 h and 24 h. Total RNA was isolated, quantified and qualified for RNA sequencing on a

NextSeq500 instrument (Illumina). A non-treated control group of DU145 cells was prepared and collected at the same time point. Approximately 7 x10^6 reads per sample were performed and a total of 46600 differentially regulated genes were detected. Differentially regulated genes were calculated using DESeq2 version 1.22.2, and selected when the expression was up- or down-regulated more than two-fold in the *C. longa* treated DU145 cells compared to the non-treated cells. We listed the general cancer-related and PCa-specific genes with top regulation scores (Log2 fold change) and $p < 0.05$. In Figure 11, the expression intensity is visualized in the heat map via a color scale, ranging between red (log2 fold change > 0, up-regulation) and green (log2 fold change < 0, down-regulation). Among the expressed genes, APLN, TIMM8A, PWP2, PMEPA1, CYR61, DKK1, FOXJ1, JUN, S100A2, ODC1, FOSL1, UPP1, and MYC were down-regulated, while p53, p21, TMEM79, ACOXL, SPINK5, NDRG1, NOTCH3, BANK1, TMEM25, INSIG1, AK7, TTLL3, SH3GL2,3, ZC3H12D, and RPS26P47 were up-regulated.

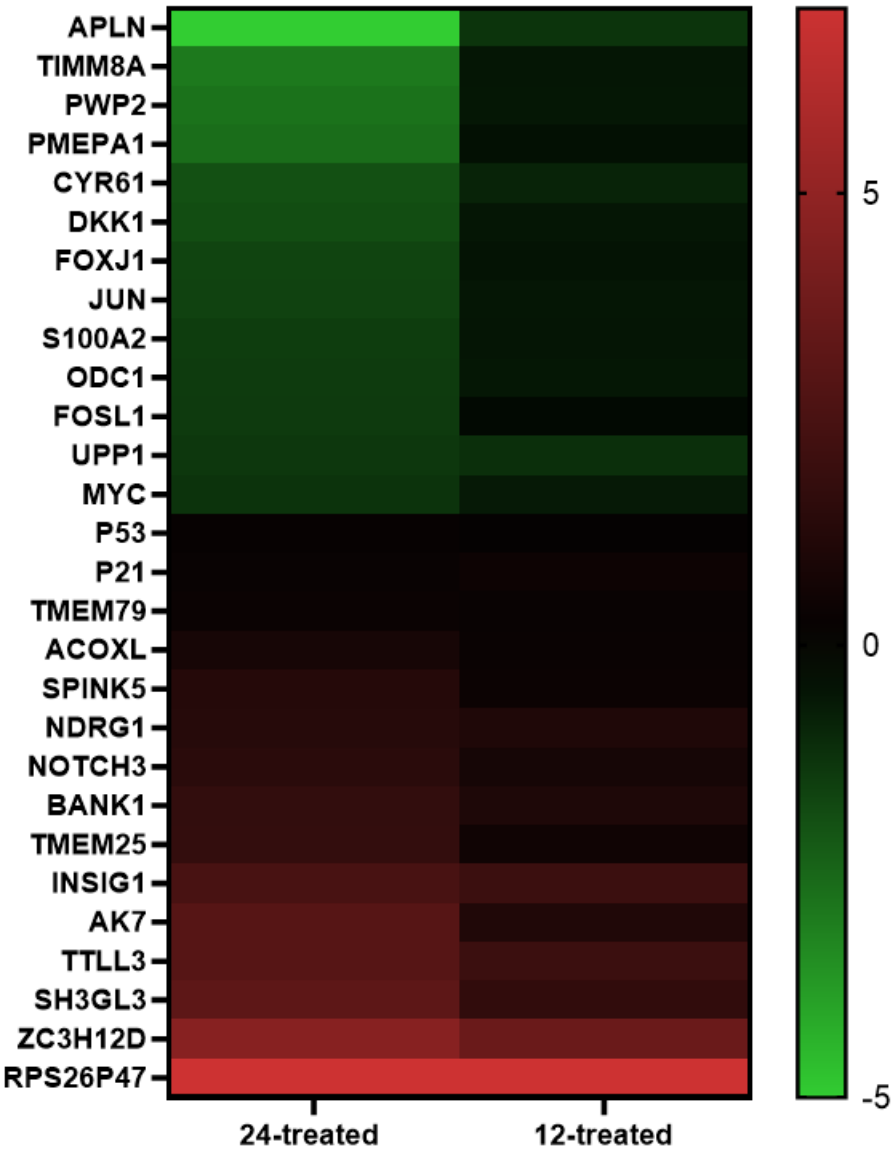

Figure 11. *C. longa* treatment regulated the expression levels of numerous cancer-related genes. An Illumina RNA sequencing was performed to detect the expression profiles of DU145 cells upon 12h or 24h *C. longa* treatment. Hierarchical analyses were performed, and the up and downstream was evaluated. APLN, TIMM8A, PWP2, PMEPA1, CYR61, DKK1, FOXJ1, JUN, S100A2, ODC1, FOSL1, UPP1, and MYC were down-regulated, while p53, p21, TMEM79, ACOXL, SPINK5, NDRG1, NOTCH3, BANK1, TMEM25, INSIG1, AK7, TTLL3, SH3GL2,3, ZC3H12D, and RPS26P47 were up-regulated.

Additionally, a volcano plot was generated, to analyze and visualize the differentially expressed genes after 24h treatment of *C. longa,* based on distance from origin via VolcaNoseR [72]. A fold change threshold between -1.1 and 1.1, and a significance threshold < 1.5 was selected, Mahattan distance was used as the criterion for ranking hits. X-axis represents log2FoldChange and Y-axis represents minus_log10_padj. The blue dots have negative fold change, meaning down-regulated genes, and the red dots positive fold change, which are up-regulated genes (Fig. 12a). Among the selected top hits, 8 genes were most related to altered cancer cell proliferation and migration, as listed in Figure 12b. ODC1, DKK1, UPP1, CYR61, FOSL1, and JUN were down-regulated, whereas INSIG1 and NDRG1 were up-regulated.

a

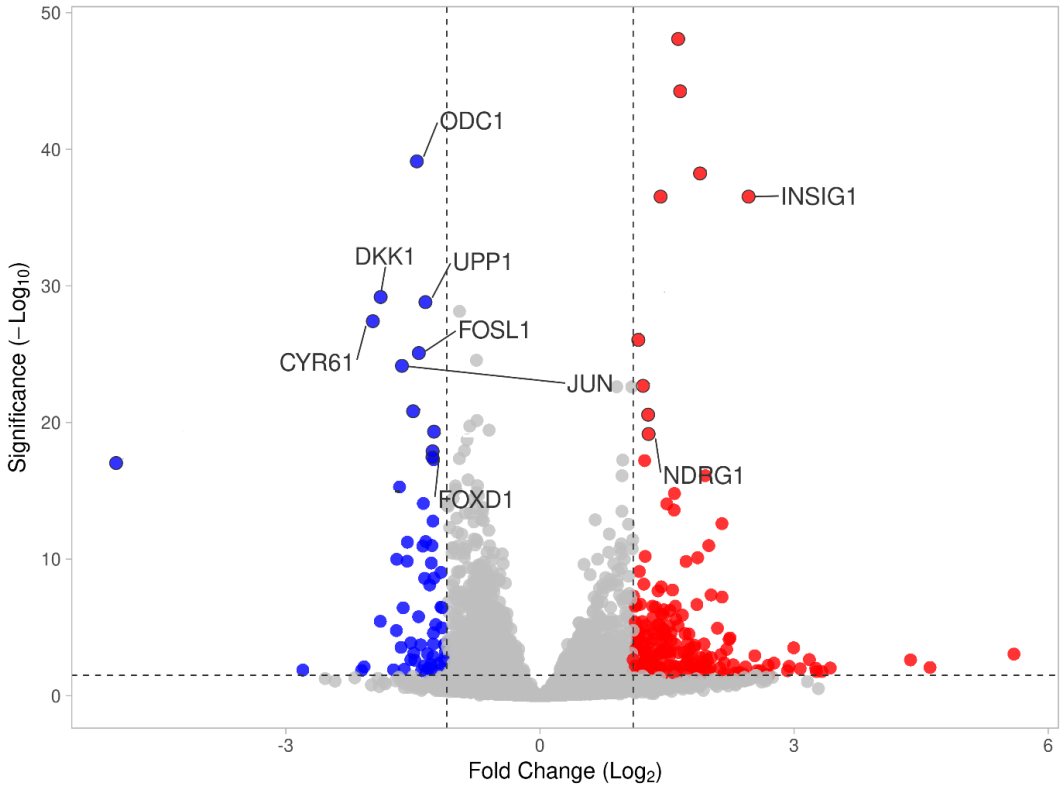

Top hits (based on distance from origin)

b

VolcaNoseR – Exploring volcano plots

Name	Change	Fold change (log2)	Significance	Manhattan distance
ODC1	Decreased	-1.453975438	39.1165	40.57047544
INSIG1	Increased	2.462604326	36.5355	38.99810433
DKK1	Decreased	-1.881095481	29.1875	31.06859548
UPP1	Decreased	-1.35225535	28.8139	30.16615535
CYR61	Decreased	-1.973133564	27.4183	29.39143356
FOSL1	Decreased	-1.430412006	25.0867	26.51711201
JUN	Decreased	-1.629656564	24.1496	25.77925656
NDRG1	Increased	1.2822102	19.1595	20.4417102

Figure 12. *C. longa* treatment regulated the expression levels of numerous cancer-related genes. (a) A volcano plot of the differentially expressed genes after 24h treatment of *C. longa* was generated via VolcaNoseR, based on distance from origin. The fold change threshold of the selected genes lies between -1.1 and 1.1, and the significance threshold < 1.5, ranked following Mahattan distance criterion. (b) Among the most cancer-related genes, an upstream of ODC1, DKK1, UPP1, CYR61, FOSL1, and JUN, and a downstream of INSIG1 and NDRG1 were obtained.

5.7 *C. longa* regulated hallmark gene sets and downstreamed regulators of the TNFα/ NFκB signaling pathway

Further analyses on the Illumina RNA sequencing results were performed, to explore the expression changes of the signaling pathways upon 24h *C. longa* treatment. A Gene Set Enrichment Analysis (GSEA) comparing the expression profiles of untreated DU145 cells with 24h treated DU145 cells, using fifty cancer-related hallmark gene sets from the Molecular Signatures Database (MSigDB) v7.5.1 was conducted via BubbleGUM (GSEA Unlimited Map) software, to detect the significant expression changes in the involving hallmark signaling at gene sets level [73, 74, 75, 76]. A significantly altered hallmark gene set embraces genes associated with the tumor necrosis factor-alpha (TNFα) signaling via NFκB, which is crucially linked to the invasion and metastasis of cancer cells (Fig. 13) [82, 83]. A volcano plot was created for visualizing the differentiated regulators (Fig. 14). NFKB1, NFκB (complex), MAP3K1, REL, and RELA, which are all important components of the TNFα/ NFκB signaling pathway, were significantly inhibited. The data shown in Figure 13 and Figure 14 indicated that, *C. longa* downstreamed the regulators and hall mark gene sets of the TNFα/ NFκB pathway.

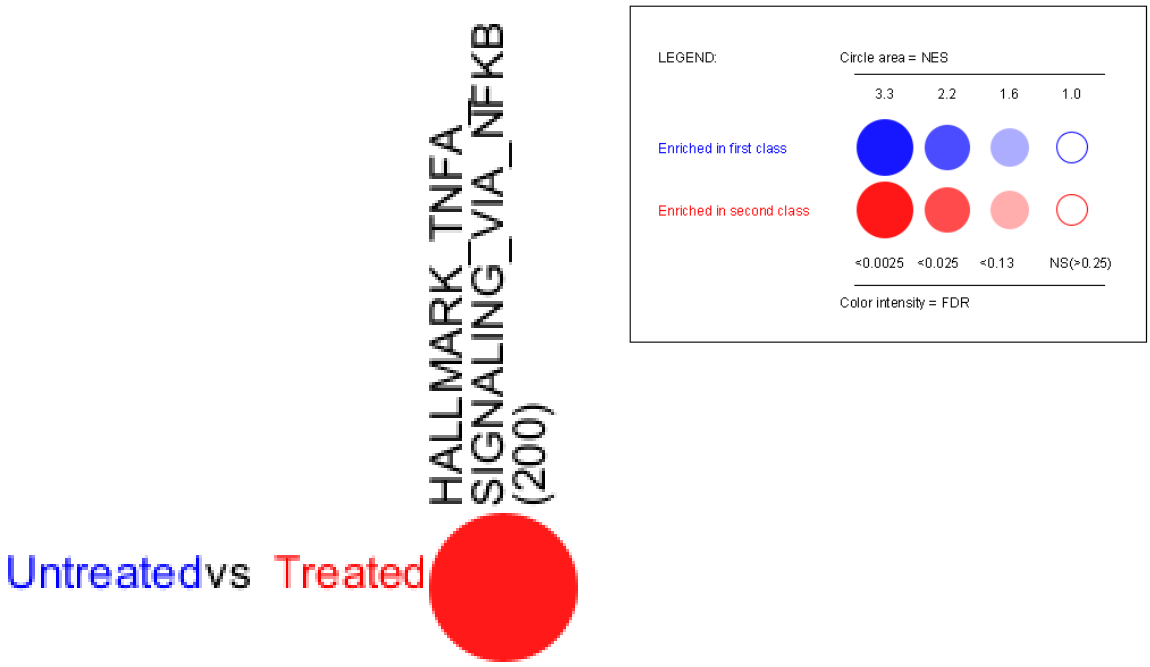

Figure 13. *C. longa* regulated gene sets associated with the TNFα/ NFκB signaling pathway. Expression profiles of 24 h treated cells and the untreated DU145 cells were compared, using fifty hallmark gene sets from the MsigDB database v7.5.1 via BubbleGUM software. The gene sets from the TNFα/ NFκB signaling pathway were enriched in the treated DU145 cells with an enrichment score of 3.3, $p < 0.0025$.

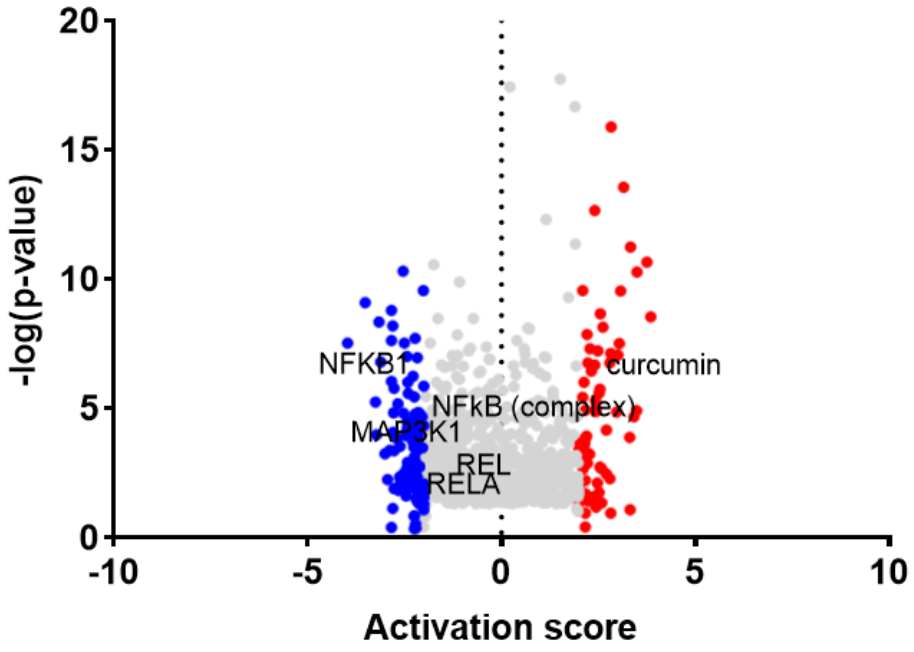

Figure 14. *C. longa* inhibited the regulators of the TNFα/ NFκB pathway. A volcano plot was created to visualize the dysregulation of the regulators after 24h *C. longa* treatment. NFKB1, NFκB (complex), MAP3K1, REL, and RELA, were significantly downregulated, with negative activation scores.

5.8 *C. longa* regulated multiple biological processes and cancer-related signaling pathways

Furthermore, the gene ontology (GO) functional annotation was analyzed based on the DAVID Bioinformatic Resources (2021 update) [77, 78]. The dysregulated pathways of biological process (BP), cellular component (CC), and molecular function (MF) were ranked based on the altered gene counts (Fig. 15). For instance, biological process pathways like negative and positive regulation of transcription, positive regulation of apoptotic process, negative regulation of cell proliferation, cholesterol biosynthesis process, response to drug, regulation of cell cycle, cellular response to TNF, Notch signaling pathway, etc., cellular component pathways including cytoplasm, membrane, endoplasmic reticulum and cell surface pathways, etc., and molecular function pathways including protein binding, receptor binding, transcription factor binding, protein C-terminus binding, protein dimerization activity, etc. are related to the pathogenic processes of cancer, and were observed to be dysregulated after 24h *C. longa* treatment.

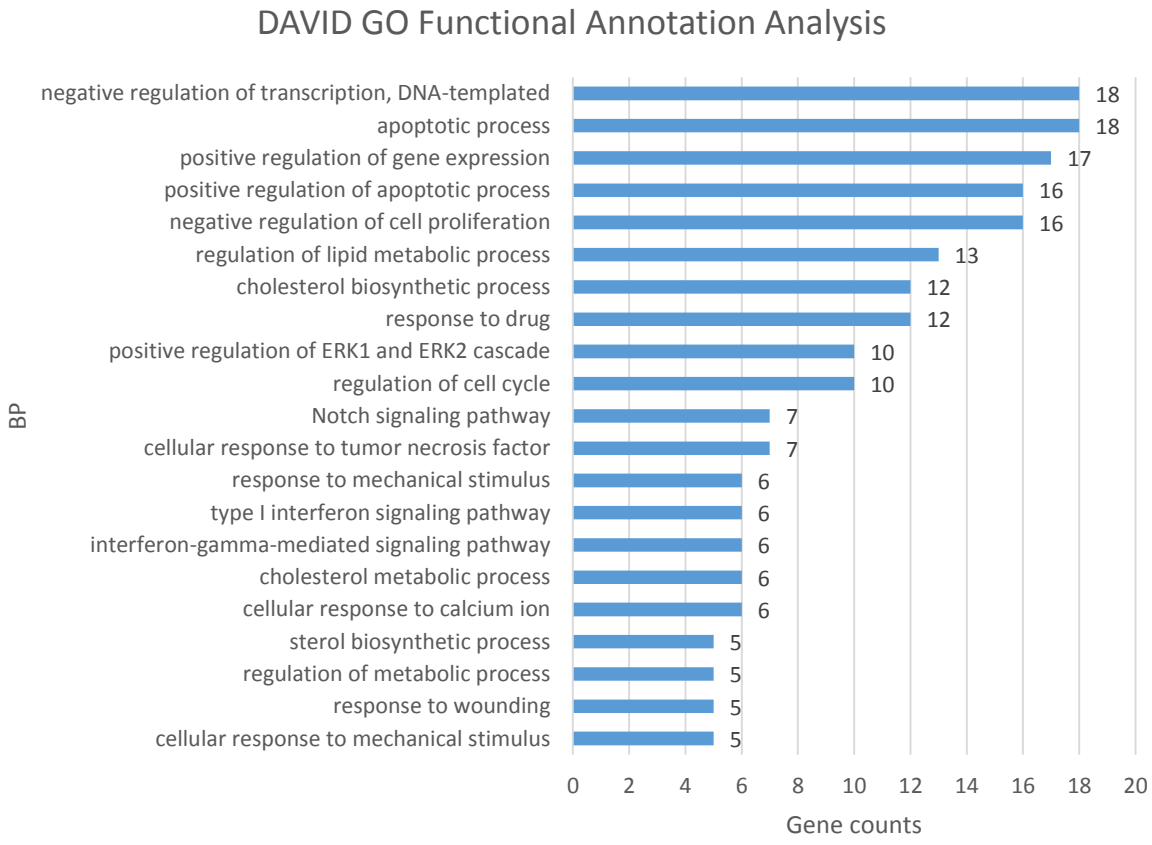

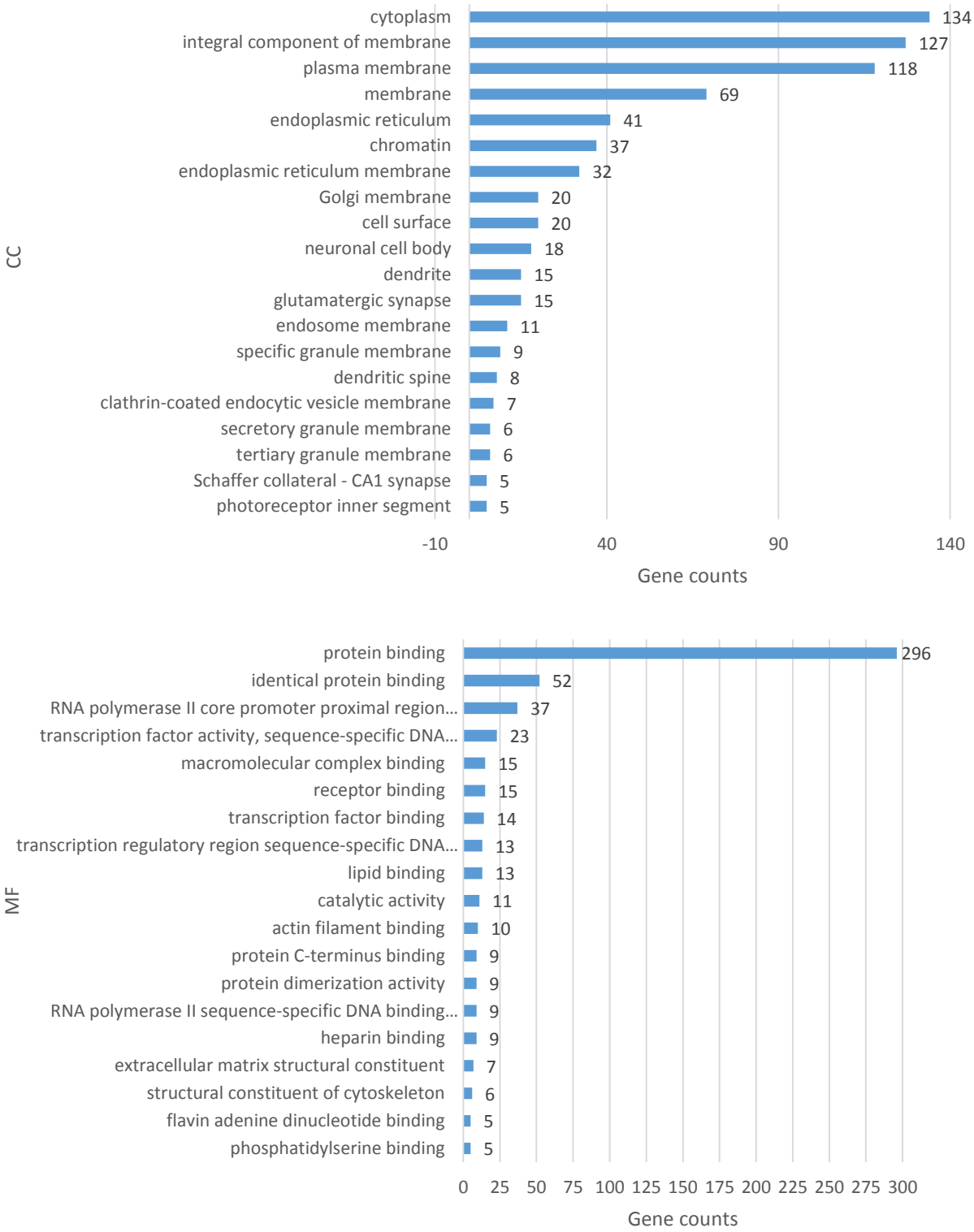

Figure 15. *C. longa* dysregulated pathways of biological process (BP), cellular component (CC), and molecular function (MF), based on the differentially expressed gene counts. The gene ontology (GO) functional annotation was analyzed based on the DAVID Bioinformatic Resources (2021 update).

Moreover, an Ingenuity Pathway Analysis (IPA) using the QIAGEN IPA (QIAGEN Inc., https://digitalinsights.qiagen.com/IPA) was performed, in order to have a precise view of the dysregulated signaling pathways, and study the relationship between multiple casual networks with various biological functions (Fig. 16) [79].

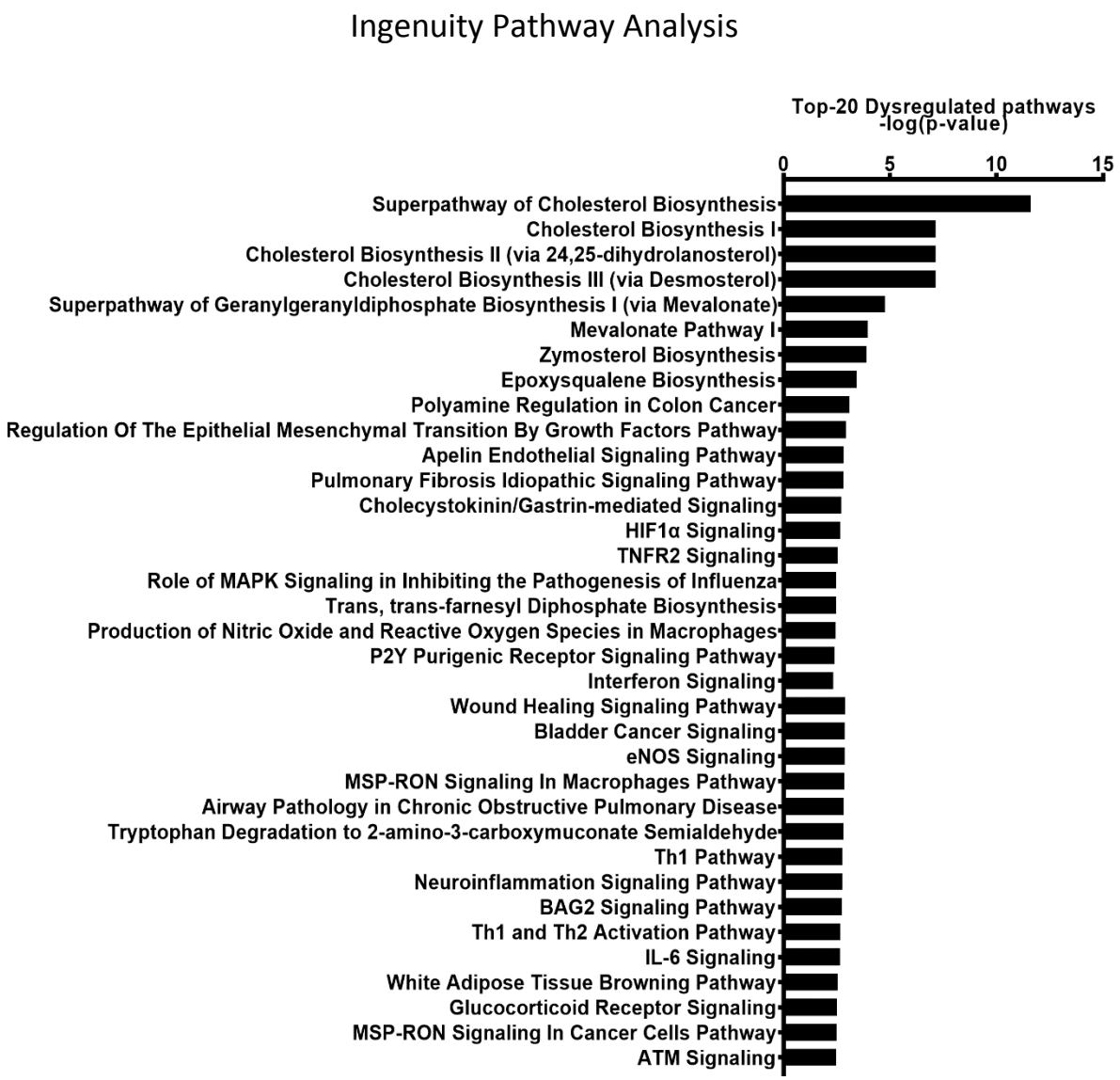

Figure 16. *C. longa* dysregulated multiple pathways of biological functions. The Ingenuity Pathway Analysis (IPA) was conducted using the QIAGEN IPA (QIAGEN Inc.). The top twenty dysregulated pathways were ranked based on –log(p-value).

6 Discussion

With the different limitations and side effects of the current treatment opportunities for PCa, complementary and alternative therapies for PCa have drawn increasing attention [2, 5, 6, 7, 8]. Moreover, the cost of the existing therapies for PCa is relative high, especially for people from developing countries, affordable therapeutic candidates using natural products with efficacy might be an option [2, 84]. The medicinal herb *C. longa* exhibits a variety of beneficial therapeutic effects, including the anticancer effect treating different types of cancer without documented risk of side effects [30]. Understanding the molecular mechanism behind the anticancer activity of *C. longa* is crucial for future animal and clinical studies.

Our study aimed to evaluate the anticancer activity of the Chinese medicinal herb Curcuma longa in human prostate cancer cells, to understand the involved mechanisms, and to discover potential biomarkers for the early diagnosis and treatment of prostate cancer. We have proved that *C. longa* has stable drug quality of temperature and pH tested with the low and high concentrations of *C. longa*. The active compounds, curcumin, bisdemethoxycurcumin, and demethoxycurcumin showed similar fingerprints in different experimental samples measured using HPLC. The characteristic peaks of the six samples remain consistent and are identical to the data of the published studies [52]. Many of the previous research focused on the isolated bioactive or synthesized components of *C. longa*, including curcumin and demethoxycurcumin [50, 51, 60, 61]. We used the whole plan extract for our study according to the original principle of Chinese traditional herbal medicine, which has used this herb for treating the diseases for thousands of years in China, Japan, Korea, as well as in many other Asian countries [85]. The world's earliest pharmacopoeia, "Tang Materia Medica", published in Chinese Tang Dynasty in 659 AD, descripted this herb for treating liver and gallbladder diseases, reducing abdomen pain and menstruation pain. *C. longa* has been described as a nontoxic herbal medicine in Chinese ancient times [41, 86]. *C. longa* and its major bioactive compound curcumin are the patent medicine in China. The evidence of many studies indicated that *C. longa* and curcumin could be developed as safe and health-beneficial drugs in Europe in the future [30, 85, 86].

In the cell viability experiments, we incubated the cells with increasing concentrations of *C. longa* to determine the most effective concentrations with the best potency. The growth of the two PCa cell lines, DU145 and PC3 were dose-dependently inhibited, while the inhibition in the control group, the human prostate epithelial cell PNT2 was observed in minuscule. At 800 µg/mL of *C. longa,* an inhibition of more than 30% was observed In DU145 cells, and an inhibition of around 25% could be observed in PC3 cells. The metastasis character of PCa cells and the sensitivity to drugs might explain the slightly different outcome between the two cell lines after *C. longa* treatment. PC3 cells have a higher metastasis and malignancy potential compared to the DU145 cells. Therefore, *C. longa* inhibited DU145 cell viability more than PC3

cell viability. We choose DU145 cell line for further experiments following the cell viability assay according to the inhibition of the viability. The inhibitory efficacy of *C. longa* was in line with other research that used isolated bioactive compounds on the same PCa cell lines, but with comparably higher concentrations ascribed to the use of whole herb extract [84, 87]. Following the cell viability assay, the mechanism behind the *C. longa*-triggered cell death was explored. DU145 cells were double-stained with annexin and PI, the apoptotic and necrotic cells were detected using FACS. The results showed that *C. longa* contributes to cell death mainly by inducing late apoptosis, with some degrees of necrosis. Therapeutic candidates with pro-apoptotic activities are preferable and have more advantages in avoiding unnecessary harm and cytotoxicity of the neighboring cells and tissues. On the contrary, necrosis may lead to inflammatory reactions and the activation of the immune response [88].

p21 and p53 genes are important players in the regulation of cancer growth [80, 89]. Being one of the earliest discovered cancer-related genes, p53 gene is closely associated with the induction of cell cycle arrest and cell apoptosis [80, 90]. For a long time, p21 was in the spotlight as a mediator of p53, showing the tumor-suppressing activity through the up-regulation of p53 gene [80]. Evidence has later accumulated that despite p53-dependent G1 growth arrest, the cyclin-dependent kinase inhibitor p21 is capable of inducing various tumor-suppressing events through multiple signaling pathways independent of p53. For instance, through binding to the cyclin dependent kinases (CDKs) and suppressing its kinase activity, p21 regulates cell cycle inhibition in response to multiple cellular stress. By binding to cyclin complexes and proliferating cell nuclear antigen (PCNA), p21 competes with DNA polymerase-δ for PCNA binding, mediates the DNA polymerase activities, and consequently suppresses DNA synthesis and thereby interfering with the DNA repair processes. Moreover, p21 regulates various gene expressions and the corresponding biological activities through protein-protein interactions, independent of CDKs and PCNA [80, 90]. p21 could also be oncogenic in certain cellular contexts, mainly due to its anti-apoptotic activity. The inhibition of apoptosis might occur in the case of post-translational modification, overexpression of p53, caspase 3 cleavage, growth factor deprivation, etc. [80, 90]. As a tumor suppressor, the expression of p21 was increased significantly at both RNA level and protein level after *C. longa* treatment in dose-dependent manners by qRT-PCR and western blot analysis. These results were confirmed by Illumina RNA sequencing analysis.

TMEM79 and ACOXL genes are reported to be two novel potential biomarkers specific for PCa, which sensitively and specifically differentiate between benign prostate gland and PCa [81]. Although the function of TMEM79 gene is not yet fully studied, it is believed that the gene is linked to several biological processes, including the maturation of the epithelial cells, the development of the epidermis, and the formation of the skin barrier function. The most

commonly known disease associated with TMEM79 is dermatitis [91, 92]. However, the differentially expressed TMEM79 in distinct types of cancer tissues implicates the possible connection of the gene with cancer. Until lately, a significant difference in the expression level between PCa tissue and normal prostate epithelial tissue has been noticed. In the cancerous tissue, a weak expression level of TMEM79 was detected, while on the contrary, normal prostate epithelial tissue contained a very strong expression level [2, 81, 92]. In the study of our colleague, microarray and western blot analysis indicate a higher intracellular expression of TMEM79 in the prostate epithelial cell line PNT2, compared to the PCa cell line DU145 [2]. Sufficient evidence has made it convincible that the positive expression level of TMEM79 is inversely linked to PCa, therefore making it a putative marker for distinguishing between benignity and tumor of the prostate [2, 81]. In the qRT-PCR and western blot analysis of our study, the expression level of TMEM79 was dose-dependently increased significantly after the treatment of *C. longa*. The function of TMEM79 in prostate tissue and the associated mechanism contributing to cancer biology still remains to be explored in future studies.

Similar to TMEM79, ACOXL was also considered to be a potential marker for identifying PCa [2, 81]. ACOXL was predicted to play a role in the regulation of acyl-CoA oxidase activity, the binding activity of flavin adenine, and lipid homeostasis, etc., although the function of the gene is not yet fully understood [93]. It is assumed that the gene participates in multiple metabolism pathways, mainly the peroxisomal lipid metabolism, and is associated with Retinitis Pigmentosa 38 [93]. Just like TMEM79, the expression level of the gene was also observed to be significantly higher in the benign prostate tissue compared to the cancerous tissue, indicating a high specificity and sensitivity of ACOXL being the marker to distinguish between benign tissue and PCa [81]. In our study, the expression level of ACOXL was increased significantly upon *C. longa* treatment dose-dependently in both RNA and protein levels, suggesting the efficacy of the treatment in bringing back the expression level to the extent of the benignancy. However, the detection of the cancer-related role and a full understanding of the functions of ACOXL is yet to be done.

RNA sequencing technology has become an essential method for whole transcriptome analysis of differential gene expression and differential splicing of mRNAs. Most of the published data of RNA sequencing used the Illumina sequencing technology [94]. In order to explore more about anticancer activity of *C. longa* in DU145 cells, to understand the mechanisms involved, to discover potential biomarkers and affected signaling pathways, and to prove the data of qRT-PCR and western blot we performed Illumina RNA sequencing to study the expression profiles of *C. longa* treated PCa cells in cooperation with the Core Facilities of the Medical University of Vienna. Among the outcome, we selected the most cancer-related especialy PCa-specific genes with top regulation scores and visualized the

expression changes after 12 h treatment and 24 h treatment using a heat map. The top eight hits were selected by significance and regulation scores following Manhattan distance, among which the cancer-promoting genes including ODC1, DKK1, UPP1, CYR61, FOSL1, and JUN were down-streamed, and the cancer-suppressing genes such as INSIG1 and NDRG1 were up-regulated.

Ornithine Decarboxylase (ODC) is the main enzyme for polyamine biosynthesis and is frequently overexpressed in multiple cancer, including prostate cancer, leading to cancer growth and is responsible for cancer aggressiveness [95, 96, 97]. Evidence proved that the inhibition of the enzyme successfully suppressed the cancer cell growth and invasiveness of PCa [97]. The Dickkopf 1 (DKK1) is an immunomodulatory protein that identifies a non-neuroendocrine subtype of mCRPC with low PSA and AR expression. It induces PCa growth and metastasis, contributing to the poor prognosis in patients with PCa [98]. In addition, DKK1 was considered to be a promising target for cancer immunotherapy, for its immune-regulatory activities [99]. Therefore, downstream of DKK1 plays a crucial role in the anticancer activities of PCa. The oncogene uridine phosphorylase 1 (UPP1) was reported to be a novel immune-related target and plays a crucial role in the malignances of several cancer types, including thyroid carcinoma, colorectal cancer, pancreatic cancer, etc [100, 101]. Although a direct correlation between UPP1 and PCa is not yet confirmed, it is accepted that UPP1 might induce similar oncogenic processes in PCa. Encoded by a growth factor inducible gene, Cysteine-rich angiogenic inducer 61 (CYR61) is overexpressed in multiple cancer with invasiveness and metastasis, including PCa [102, 103]. CYR61 expression is linked to the chance of disease reoccurrence and was therefore suggested to be a potential prognostic marker for PCa [104]. The Fos-like gene FOSL1 is highly expressed in PCa, enhancing PCa cell growth and metastasis [105]. Studies indicated that FOSL1 induces the tumorigenic processes through the epithelial mesenchymal transition pathway [105]. Additionally, FOSL1 gene is capable of dimerization with JUN genes, forming the activating protein-1 (AP1) complex, which is responsible for the regulation of cancer cell proliferation, and cell differentiation [106]. Being a family member of the AP1 protein, the JUN proto-oncogene is involved in various tumorigenic signaling pathways, such as the NFκB pathway and different apoptotic pathways. The downstream of these cancer-promoting genes indicates the anticancer efficacy of *C. longa* [107].

The up-regulation of the tumor-suppressing genes INSIG1 and NDRG1 might bring us some implications for the anticancer property of *C. longa*. Excessive cholesterol biosynthesis is a disease hallmark in many types of cancer, including PCa [108]. The insulin-induced gene 1 (INSIG1), a cholesterol biosynthesis modulator, was reported to suppress tumor proliferation and migration in hepatocellular carcinoma through the regulation of hypoxia. In addition, the

gene was also documented to play a role in breast cancer and gastric cancer [109]. With cholesterol level being a crucial risk of the aggressive PCa, it could be accepted that INSIG1 is involved in the regulation of the PCa pathogenesis. The prostate metastasis suppressor N-myc downregulated gene 1 (NDRG1) mediates androgen receptor signaling by inhibiting both androgen-dependent and independent activation of AR expression [110]. Apart from this, the gene is also involved in the growth, survival, and metastasis of cancer cells, and is therefore a putative therapeutic target and biomarker of PCa [110]. Both INSIG and NDRG1 play crucial roles in cancer-related events in PCa, thus the upstream of the two genes indicates promising anticancer activities of *C. longa* [108, 110]

By comparing the dysregulated hallmark and the mediated regulators, we observed the significant differentiation of the TNFα/ NFκB signaling pathway. The tumor necrosis factor-alpha (TNFα) has a key role in establishing a connection between inflammatory reactions and cancer and participates in various tumorigenic processes, including cancer cell proliferation, transformation, and invasion [111]. The key regulating role of TNFα in tumor microenvironment is often linked to the pathway with NFκB. Nuclear factor-κB (NFκB) is a transcription factor family with a wide range of gene targets and regulates multiple immune processes [112, 113]. Structurally, NFκB consists of NFκB1 (p50), NFκB2 (p52), RelA (p65), RelB, and c-Rel, each of which is capable of forming homodimeric or heterodimeric complexes, involved in various functional signaling [113, 114]. The activation of NFκB upon the binding of TNFα to its receptor TNFR1 is crucial for TNFα-induced cancer cell survival and proliferation. The activation and the signaling pathway of NFκB is rather complicated, here we only focus on a small part of the cancer-inducing aspect of the NFκB signaling [112, 113, 114]. According to our data analysis, the NFκB complex along with some of its structural components and the gene targets of the TNFα/ NFκB signaling pathway were down-regulated, suggesting a downstream of the tumor-promoting pathway after the treatment.

Last but not the least, we performed GO analysis to explore the function, location, and the probable associated biological processes of the differentially expressed genes. The aim of this approach is to identify the putative gene targets and possible mechanisms, and provide the additional knowledge for future studies.

Our finding has provided experimental evidence for the medicinal herb *C. longa* as a safe and effective candidate for the inhibition of cell growth and metastasis in PCa. It also provided some aspects of the possible molecular mechanism behind the tumor-suppressing activity and brought some pharmaceutical implications of using safe herbal extracts as a complementary therapeutic option. However, the pathogenesis of PCa is extremely complicated with numerous gene regulators and a full understanding of the mechanism is still urgently required.

In conclusion, our study demonstrated that the extracts from the medicinal plant *C. longa* maintained good thermal and pH stability during the experimental procedures and showed good quality as indicated by nearly identical fingerprints among the different experimental samples. They could potentially be developed as a safe and effective beneficiary candidate playing a complementary or alternative role for treating PCa.

Our results showed that *C. longa* inhibited the proliferation of DU145 cells and suppressed their cell viability compared with PNT2 cells. qRT-PCR and western blot analysis demonstrated that *C. longa* up-regulated the expression levels of p21, TMEM79, and ACOXL significantly. These results were confirmed by Illumina RNA sequencing analysis. The data analysis of RNA sequencing detected a total of 46600 differentially regulated genes. Among them, ODC1, DKK1, UPP1, CYR61, FOSL1, and JUN were up-regulated significantly, while INSIG1 and NDRG1 were down-regulated significantly. *C. longa* inhibited the regulators and hallmark gene sets of the TNFα/NFκB signaling pathway as well as other cancer-related signaling pathways pointing that *C. longa* could be novel candidate for PCa research in the future.

7 Limitations

Our study has some limitations.

We used whole plant extracts for this investigation. As a next step, we should perform a comparison study with the plant extract and its main active compounds.

We performed cellular experiments with the PCa cell lines. We should evaluate the anticancer activities after *C. longa* treatment in different immune cells.

The Illumina RNA sequencing data provided us with more details of the genome-wide expression profiles in the treated cells. From RNA sequencing we obtained a lot of regulatory genes and mediated pathways, which need further investigations to prove and discuss the involved mechanisms in future studies.

8 References

1. AUSTRIA, STATISTIK. 2022. "Krebserkrankungen". *Statistik.At*. https://www.statistik.at/web_de/statistiken/menschen_und_gesellschaft/gesundheit/krebserkrankungen/index.html.
2. He, Shan, Fangqiao Lyu, Lixia Lou, Lu Liu, Songlin Li, Johannes Jakowitsch, and Yan Ma. 2021. "Anti-Tumor Activities Of Panax Quinquefolius Saponins And Potential Biomarkers In Prostate Cancer". *Journal Of Ginseng Research* 45 (2): 273-286. doi:10.1016/j.jgr.2019.12.007.
3. Teo, Min Yuen, Dana E. Rathkopf, and Philip Kantoff. 2019. "Treatment Of Advanced Prostate Cancer". *Annual Review Of Medicine* 70 (1): 479-499. doi:10.1146/annurev-med-051517-011947.
4. Evans, Andrew J. 2018. "Treatment Effects In Prostate Cancer". *Modern Pathology* 31 (S1): 110-121. doi:10.1038/modpathol.2017.158.
5. Thompson, Ian M. 2005. "Operating Characteristics Of Prostate-Specific Antigen In Men With An Initial PSA Level Of 3.0 Ng/Ml Or Lower". *JAMA* 294 (1): 66. doi:10.1001/jama.294.1.66.
6. Carter, H. Ballentine. 2004. "Prostate Cancers In Men With Low PSA Levels — Must We Find Them?". *New England Journal Of Medicine* 350 (22): 2292-2294. doi:10.1056/nejme048003.
7. Sebesta, Elisabeth M., and Christopher B. Anderson. 2017. "The Surgical Management Of Prostate Cancer". *Seminars In Oncology* 44 (5): 347-357. doi:10.1053/j.seminoncol.2018.01.003.
8. Ahdoot, Michael, Amir H. Lebastchi, Baris Turkbey, Bradford Wood, and Peter A. Pinto. 2019. "Contemporary Treatments In Prostate Cancer Focal Therapy". *Current Opinion In Oncology* 31 (3): 200-206. doi:10.1097/cco.0000000000000515.
9. Lopez, William, Nhu Nguyen, Jessica Cao, Christine Eddow, K. Kirk Shung, Nan Sook Lee, and Mosses S. S. Chow. 2021. "Ultrasound Therapy, Chemotherapy And Their Combination For Prostate Cancer". *Technology In Cancer Research & Treatment* 20: 153303382110119. doi:10.1177/15330338211011965.
10. Carles, Joan, Daniel Castellano, Miguel Ángel Climent, Pablo Maroto, Rafael Medina, and Antonio Alcaraz. 2012. "Castration-Resistant Metastatic Prostate Cancer: Current Status And Treatment Possibilities". *Clinical And Translational Oncology* 14 (3): 169-176. doi:10.1007/s12094-012-0780-8.
11. Yang, Lei, Changqing Yang, Chenyi Li, Qing Zhao, Ling Liu, Xin Fang, and Xiao-Ya Chen. 2016. "Recent Advances In Biosynthesis Of Bioactive Compounds In Traditional

Chinese Medicinal Plants". *Science Bulletin* 61 (1): 3-17. doi:10.1007/s11434-015-0929-2.

12. Kaya, Pelin, Sang Lee, Young Lee, Sun Kwon, Hyun Yang, Hye Lee, and Eui-Ju Hong. 2019. "Curcumae Radix Extract Decreases Mammary Tumor-Derived Lung Metastasis Via Suppression Of C-C Chemokine Receptor Type 7 Expression". *Nutrients* 11 (2): 410. doi:10.3390/nu11020410.
13. Zheng, Jie, Yue Zhou, Ya Li, Dong-Ping Xu, Sha Li, and Hua-Bin Li. 2016. "Spices For Prevention And Treatment Of Cancers". *Nutrients* 8 (8): 495. doi:10.3390/nu8080495.
14. Zhao, Wanli, Xudong Zhou, Guisong Qi, and Yuexian Guo. 2018. "Curcumin Suppressed The Prostate Cancer By Inhibiting JNK Pathways Via Epigenetic Regulation". *Journal Of Biochemical And Molecular Toxicology* 32 (5): e22049. doi:10.1002/jbt.22049.
15. Merriel, Samuel W. D., Garth Funston, and Willie Hamilton. 2018. "Prostate Cancer In Primary Care". *Advances In Therapy* 35 (9): 1285-1294. doi:10.1007/s12325-018-0766-1.
16. Hamilton, W, A Round, D Sharp, and T J Peters. 2005. "Clinical Features Of Colorectal Cancer Before Diagnosis: A Population-Based Case–Control Study". *British Journal Of Cancer* 93 (4): 399-405. doi:10.1038/sj.bjc.6602714.
17. "Prostate Cancer Signs And Symptoms". 2022. *Amp.Cancer.Org*. https://amp.cancer.org/cancer/prostate-cancer/detection-diagnosis-staging/signs-symptoms.html.
18. Adhyam, Mohan, and Anish Kumar Gupta. 2012. "A Review On The Clinical Utility Of PSA In Cancer Prostate". *Indian Journal Of Surgical Oncology* 3 (2): 120-129. doi:10.1007/s13193-012-0142-6.
19. "Prostate Cancer: Age-Specific Screening Guidelines". 2022. *Hopkinsmedicine.Org*. https://www.hopkinsmedicine.org/health/conditions-and-diseases/prostate-cancer/prostate-cancer-age-specific-screening-guidelines.
20. "Prostate-Specific Antigen (PSA) Test". 2022. *National Cancer Institute*. https://www.cancer.gov/types/prostate/psa-fact-sheet.
21. Merriel, Samuel W. D., Garth Funston, and Willie Hamilton. 2018. "Prostate Cancer In Primary Care". *Advances In Therapy* 35 (9): 1285-1294. doi:10.1007/s12325-018-0766-1.
22. Chen, Ronald C., R. Bryan Rumble, and Suneil Jain. 2016. "Active Surveillance For The Management Of Localized Prostate Cancer (Cancer Care Ontario Guideline): American Society Of Clinical Oncology Clinical Practice Guideline Endorsement Summary". *Journal Of Oncology Practice* 12 (3): 267-269. doi:10.1200/jop.2015.010017.

23. Wang, Guocan, Di Zhao, Denise J. Spring, and Ronald A. DePinho. 2018. "Genetics And Biology Of Prostate Cancer". *Genes & Development* 32 (17-18): 1105-1140. doi:10.1101/gad.315739.118.
24. Zaorsky, Nicholas G., Brian J. Davis, Paul L. Nguyen, Timothy N. Showalter, Peter J. Hoskin, Yasuo Yoshioka, Gerard C. Morton, and Eric M. Horwitz. 2017. "The Evolution Of Brachytherapy For Prostate Cancer". *Nature Reviews Urology* 14 (7): 415-439. doi:10.1038/nrurol.2017.76.
25. Costello, Anthony J. 2020. "Considering The Role Of Radical Prostatectomy In 21St Century Prostate Cancer Care". *Nature Reviews Urology* 17 (3): 177-188. doi:10.1038/s41585-020-0287-y.
26. Ingrosso, Gianluca, Beatrice Detti, Daniele Scartoni, Andrea Lancia, Irene Giacomelli, Muhammed Baki, Giulio Carta, Lorenzo Livi, and Riccardo Santoni. 2018. "Current Therapeutic Options In Metastatic Castration-Resistant Prostate Cancer". *Seminars In Oncology* 45 (5-6): 303-315. doi:10.1053/j.seminoncol.2018.10.001.
27. Gamat, Melissa, and Douglas G McNeel. 2017. "Androgen Deprivation And Immunotherapy For The Treatment Of Prostate Cancer". *Endocrine-Related Cancer* 24 (12): T297-T310. doi:10.1530/erc-17-0145.
28. Namekawa, Takeshi, Kazuhiro Ikeda, Kuniko Horie-Inoue, and Satoshi Inoue. 2019. "Application Of Prostate Cancer Models For Preclinical Study: Advantages And Limitations Of Cell Lines, Patient-Derived Xenografts, And Three-Dimensional Culture Of Patient-Derived Cells". *Cells* 8 (1): 74. doi:10.3390/cells8010074.
29. Cha, Ha-Ram, Joo Hyoung Lee, and Selvarangan Ponnazhagan. 2020. "Revisiting Immunotherapy: A Focus On Prostate Cancer". *Cancer Research* 80 (8): 1615-1623. doi:10.1158/0008-5472.can-19-2948.
30. 2022.*Ema.Europa.Eu*. https://www.ema.europa.eu/en/medicines/herbal/curcumae-longae-rhizoma.
31. Saranyutanon, Sirin, Sanjeev Kumar Srivastava, Sachin Pai, Seema Singh, and Ajay Pratap Singh. 2019. "Therapies Targeted To Androgen Receptor Signaling Axis In Prostate Cancer: Progress, Challenges, And Hope". *Cancers* 12 (1): 51. doi:10.3390/cancers12010051.
32. Rybak, Adrian P., Robert G. Bristow, and Anil Kapoor. 2014. "Prostate Cancer Stem Cells: Deciphering The Origins And Pathways Involved In Prostate Tumorigenesis And Aggression". *Oncotarget* 6 (4): 1900-1919. doi:10.18632/oncotarget.2953.
33. Namekawa, Takeshi, Kazuhiro Ikeda, Kuniko Horie-Inoue, and Satoshi Inoue. 2019. "Application Of Prostate Cancer Models For Preclinical Study: Advantages And Limitations Of Cell Lines, Patient-Derived Xenografts, And Three-Dimensional Culture Of Patient-Derived Cells". *Cells* 8 (1): 74. doi:10.3390/cells8010074.

34. "Lncap Cells: Transfection And Lncap Cell Culture Protocols". 2022. *Lncap Cell Line* -. http://www.lncap.com/.
35. Tai, Sheng, Yin Sun, Jill M. Squires, Hong Zhang, William K. Oh, Chao-Zhao Liang, and Jiaoti Huang. 2011. "PC3 Is A Cell Line Characteristic Of Prostatic Small Cell Carcinoma". *The Prostate* 71 (15): 1668-1679. doi:10.1002/pros.21383.
36. Stone, Kenneth R., Don D. Mickey, Heidi Wunderli, George H. Mickey, and David F. Paulson. 1978. "Isolation Of A Human Prostate Carcinoma Cell Line (DU 145)". *International Journal Of Cancer* 21 (3): 274-281. doi:10.1002/ijc.2910210305.
37. Nguyen, Holly M., Robert L. Vessella, Colm Morrissey, Lisha G. Brown, Ilsa M. Coleman, Celestia S. Higano, and Elahe A. Mostaghel et al. 2017. "Lucap Prostate Cancer Patient-Derived Xenografts Reflect The Molecular Heterogeneity Of Advanced Disease AnD Serve As Models For Evaluating Cancer Therapeutics". *The Prostate* 77 (6): 654-671. doi:10.1002/pros.23313.
38. Foglietta, Federica, Roberto Canaparo, Giampiero Muccioli, Enzo Terreno, and Loredana Serpe. 2020. "Methodological Aspects And Pharmacological Applications Of Three-Dimensional Cancer Cell Cultures And Organoids". *Life Sciences* 254: 117784. doi:10.1016/j.lfs.2020.117784.
39. Niemeyer, Kathryn, Iris R. Bell, and Mary Koithan. 2013. "Traditional Knowledge Of Western Herbal Medicine And Complex Systems Science". *Journal Of Herbal Medicine* 3 (3): 112-119. doi:10.1016/j.hermed.2013.03.001.
40. Unschuld, Paul Ulrich (1986), Medicine in China, A History of Pharmaceutics, 本草, University of California Press.
41. Tang Ben Cao 唐本草 , Su et.al, 659 AD
42. Tu, Youyou. 2016. "Artemisinin-A Gift From Traditional Chinese Medicine To The World (Nobel Lecture)". *Angewandte Chemie International Edition* 55 (35): 10210-10226. doi:10.1002/anie.201601967.
43. Chandrasekaran, ChinampudurV et al. 2013. "Immune-stimulatory and anti-inflammatory activities of Curcuma longa extract and its polysaccharide fraction". Pharmacognosy Research 5 (2): 71. Medknow. doi:10.4103/0974-8490.110527.
44. Ma H, Chen G, Pei YH. 2013. Isolation and identification of chemical con-stituents from rhizoma ofCoptis chinensisand their cytotoxic activities. JShenyang Pharm Univ. 63:1–9.
45. Wang, Jigang, Chengchao Xu, Yin Kwan Wong, Yujie Li, Fulong Liao, Tingliang Jiang, and Youyou Tu. 2019. "Artemisinin, The Magic Drug Discovered From Traditional Chinese Medicine". *Engineering* 5 (1): 32-39. doi:10.1016/j.eng.2018.11.011.

46. Hong. 2009. "Berberine inhibits p53-dependent cell growth through induction of apoptosis of prostate cancer cells". International Journal of Oncology. Spandidos Publications. doi:10.3892/ijo_00000250.
47. Peng & Xiang-Bo Yang (2019) Coptidis Rhizoma: a comprehensive review of its traditionaluses, botany, phytochemistry, pharmacology and toxicology, Pharmaceutical Biology, 57:1,193-225, DOI: 10.1080/13880209.2019.1577466
48. Zhao, Wanli et al. 2018. "Curcumin suppressed the prostate cancer by inhibiting JNK pathways via epigenetic regulation". *Journal of Biochemical and Molecular Toxicology* 32 (5): e22049. Wiley. doi:10.1002/jbt.22049.
49. Rao, K.V.K. et al. 2012. "Chemopreventive Potential of an Ethyl Acetate Fraction from Curcuma Longa is Associated with Upregulation of p57kip2and Rad9 in the PC-3M Prostate Cancer Cell Line". *Asian Pacific Journal of Cancer Prevention* 13 (3): 1031-1038. Asian Pacific Organization for Cancer Prevention. doi:10.7314/apjcp.2012.13.3.1031.
50. Yu, Xiao-Ling et al. 2014. "Curcumin Inhibits Expression of Inhibitor of DNA Binding 1 in PC3 Cells and Xenografts". *Asian Pacific Journal of Cancer Prevention* 15 (3): 1465-1470. Asian Pacific Organization for Cancer Prevention. doi:10.7314/apjcp.2014.15.3.1465.
51. Katta, Shilpa et al. 2019. "Curcumin-Gene Expression Response in Hormone Dependent and Independent Metastatic Prostate Cancer Cells". *International Journal of Molecular Sciences* 20 (19): 4891. MDPI AG. doi:10.3390/ijms20194891.
52. Pan, Yan, Ronghui Ju, Xueli Cao, Hairun Pei, Tianhao Zheng, and Wei Wang. 2020. "Optimization Extraction And Purification Of Biological Activity Curcumin From <I>Curcuma Longa</I> L By High-Performance Counter-Current Chromatography". *Journal Of Separation Science* 43 (8): 1586-1592. doi:10.1002/jssc.201901174.
53. Ru, Jinlong, Peng Li, Jinan Wang, Wei Zhou, Bohui Li, Chao Huang, and Pidong Li et al. 2014. "TCMSP: A Database Of Systems Pharmacology For Drug Discovery From Herbal Medicines". *Journal Of Cheminformatics* 6 (1). doi:10.1186/1758-2946-6-13.
54. Grindstad, Thea, Elin Richardsen, Sigve Andersen, Kaja Skjefstad, Mehrdad Rakaee khanehkenari, Tom Donnem, and Nora Ness et al. 2018. "Progesterone Receptors In Prostate Cancer: Progesterone Receptor B Is The Isoform Associated With Disease Progression". *Scientific Reports* 8 (1). doi:10.1038/s41598-018-29520-5.
55. Chung, Wen-Cheng, Xinchun Zhou, Azeddine Atfi, and Keli Xu. 2020. "PIK3CG Is A Potential Therapeutic Target In Androgen Receptor–Indifferent Metastatic Prostate Cancer". *The American Journal Of Pathology* 190 (11): 2194-2202. doi:10.1016/j.ajpath.2020.07.013.

56. Qin, Jun, Hui-Ju Lee, San-Pin Wu, Shih-Chieh Lin, Rainer B. Lanz, Chad J. Creighton, Francesco J. DeMayo, Sophia Y. Tsai, and Ming-Jer Tsai. 2014. "Androgen Deprivation–Induced Ncoa2 Promotes Metastatic And Castration-Resistant Prostate Cancer". *Journal Of Clinical Investigation* 124 (11): 5013-5026. doi:10.1172/jci76412.
57. Yang, Shouhui, Peijun He, Jian Wang, Aaron Schetter, Wei Tang, Naotake Funamizu, and Katsuhiko Yanaga et al. 2016. "A Novel MIF Signaling Pathway Drives The Malignant Character Of Pancreatic Cancer By Targeting NR3C2". *Cancer Research* 76 (13): 3838-3850. doi:10.1158/0008-5472.can-15-2841.
58. Tuttle, Traci R., Michelle L. Mierzwa, Susanne I. Wells, Sejal R. Fox, and Nira Ben-Jonathan. 2016. "The Cyclic GMP/Protein Kinase G Pathway As A Therapeutic Target In Head And Neck Squamous Cell Carcinoma". *Cancer Letters* 370 (2): 279-285. doi:10.1016/j.canlet.2015.10.024.
59. Bong, Alice H.L., and Gregory R. Monteith. 2018. "Calcium Signaling And The Therapeutic Targeting Of Cancer Cells". *Biochimica Et Biophysica Acta (BBA) - Molecular Cell Research* 1865 (11): 1786-1794. doi:10.1016/j.bbamcr.2018.05.015.
60. Chaudhary, Lala R. & Hruska, Keith A. 2003. "Inhibition of cell survival signal protein kinase B/Akt by curcumin in human prostate cancer cells". *Journal of Cellular Biochemistry* 89 (1): 1-5. Wiley. doi:10.1002/jcb.10495.
61. Ide, Hisamitsu et al. 2018. "Modulation of AKR1C2 by curcumin decreases testosterone production in prostate cancer". *Cancer Science* 109 (4): 1230-1238. Wiley. doi:10.1111/cas.13517
62. Choi, H Y; Lim, J E & Hong, J H. 2010. "Curcumin interrupts the interaction between the androgen receptor and Wnt/β-catenin signaling pathway in LNCaP prostate cancer cells". *Prostate Cancer and Prostatic Diseases* 13 (4): 343-349. Springer Science and Business Media LLC. doi:10.1038/pcan.2010.26.
63. Liu, He et al. 2018. "H3K4me3 and Wdr82 are associated with tumor progression and a favorable prognosis in human colorectal cancer". *Oncology Letters*. Spandidos Publications. doi:10.3892/ol.2018.8902.
64. Srivastava, Rakesh K. et al. 2007. "Linkage of Curcumin-Induced Cell Cycle Arrest and Apoptosis by Cyclin-Dependent Kinase Inhibitor p21/WAF1/CIP1". *Cell Cycle* 6 (23): 2953-2961. Informa UK Limited. doi:10.4161/cc.6.23.4951.
65. Hong, J H et al. 2006. "The effects of curcumin on the invasiveness of prostate cancer in vitro and in vivo". *Prostate Cancer and Prostatic Diseases* 9 (2): 147-152. Springer Science and Business Media LLC. doi:10.1038/sj.pcan.4500856.
66. Cheng, T.-S. et al. 2013. "Curcumin-Targeting Pericellular Serine Protease Matriptase Role in Suppression of Prostate Cancer Cell Invasion, Tumor Growth, and Metastasis".

Cancer Prevention Research 6 (5): 495-505. American Association for Cancer Research (AACR). doi:10.1158/1940-6207.capr-12-0293-t.

67. Martin, Marcel. 2011. "Cutadapt Removes Adapter Sequences From High-Throughput Sequencing Reads". *Embnet.Journal* 17 (1): 10. doi:10.14806/ej.17.1.200.
68. GRCh38 human reference genome downloaded from NCBI (2018-09-27): ftp://ftp.ncbi.nlm.nih.gov/genomes/all/GCA/000/001/405/GCA_000001405.15_GRCh38/seqs_for_alignment_pipelines.ucsc_ids/GCA_000001405.15_GRCh38_no_alt_analysis_set.fna.gz
69. Human genome annotations downloaded from Gencode (2018-11-22): ftp://ftp.ebi.ac.uk/pub/databases/gencode/Gencode_human/release_29/gencode.v29.chr_patch_hapl_scaff.annotation.gtf.gz
70. Dobin, Alexander, Carrie A. Davis, Felix Schlesinger, Jorg Drenkow, Chris Zaleski, Sonali Jha, Philippe Batut, Mark Chaisson, and Thomas R. Gingeras. 2012. "STAR: Ultrafast Universal RNA-Seq Aligner". *Bioinformatics* 29 (1): 15-21. doi:10.1093/bioinformatics/bts635.
71. Love, Michael I, Wolfgang Huber, and Simon Anders. 2014. "Moderated Estimation Of Fold Change And Dispersion For RNA-Seq Data With Deseq2". *Genome Biology* 15 (12). doi:10.1186/s13059-014-0550-8.
72. Goedhart, Joachim, and Martijn S. Luijsterburg. 2020. "Volcanoser Is A Web App For Creating, Exploring, Labeling And Sharing Volcano Plots". *Scientific Reports* 10 (1). doi:10.1038/s41598-020-76603-3.
73. Subramanian, Aravind, Pablo Tamayo, Vamsi K. Mootha, Sayan Mukherjee, Benjamin L. Ebert, Michael A. Gillette, and Amanda Paulovich et al. 2005. "Gene Set Enrichment Analysis: A Knowledge-Based Approach For Interpreting Genome-Wide Expression Profiles". *Proceedings Of The National Academy Of Sciences* 102 (43): 15545-15550. doi:10.1073/pnas.0506580102.
74. Liberzon, A., A. Subramanian, R. Pinchback, H. Thorvaldsdottir, P. Tamayo, and J. P. Mesirov. 2011. "Molecular Signatures Database (Msigdb) 3.0". *Bioinformatics* 27 (12): 1739-1740. doi:10.1093/bioinformatics/btr260.
75. Liberzon, Arthur, Chet Birger, Helga Thorvaldsdóttir, Mahmoud Ghandi, Jill P. Mesirov, and Pablo Tamayo. 2015. "The Molecular Signatures Database Hallmark Gene Set Collection". *Cell Systems* 1 (6): 417-425. doi:10.1016/j.cels.2015.12.004.
76. Spinelli, Lionel, Sabrina Carpentier, Frédéric Montañana Sanchis, Marc Dalod, and Thien-Phong Vu Manh. 2015. "Bubblegum: Automatic Extraction Of Phenotype Molecular Signatures And Comprehensive Visualization Of Multiple Gene Set Enrichment Analyses". *BMC Genomics* 16 (1). doi:10.1186/s12864-015-2012-4.

77. Huang, Da Wei, Brad T Sherman, and Richard A Lempicki. 2008. "Systematic And Integrative Analysis Of Large Gene Lists Using DAVID Bioinformatics Resources". *Nature Protocols* 4 (1): 44-57. doi:10.1038/nprot.2008.211.
78. Huang, Da Wei, Brad T. Sherman, and Richard A. Lempicki. 2008. "Bioinformatics Enrichment Tools: Paths Toward The Comprehensive Functional Analysis Of Large Gene Lists". *Nucleic Acids Research* 37 (1): 1-13. doi:10.1093/nar/gkn923.
79. Krämer, Andreas, Jeff Green, Jack Pollard, and Stuart Tugendreich. 2013. "Causal Analysis Approaches In Ingenuity Pathway Analysis". *Bioinformatics* 30 (4): 523-530. doi:10.1093/bioinformatics/btt703.
80. Abbas, Tarek, and Anindya Dutta. 2009. "P21 In Cancer: Intricate Networks And Multiple Activities". *Nature Reviews Cancer* 9 (6): 400-414. doi:10.1038/nrc2657.
81. O'Hurley, Gillian, Christer Busch, Linn Fagerberg, Björn M. Hallström, Charlotte Stadler, Anna Tolf, and Emma Lundberg et al. 2015. "Analysis Of The Human Prostate-Specific Proteome Defined By Transcriptomics And Antibody-Based Profiling Identifies TMEM79 And ACOXL As Two Putative, Diagnostic Markers In Prostate Cancer". *PLOS ONE* 10 (8): e0133449. doi:10.1371/journal.pone.0133449.
82. Wu, Y, and B P Zhou. 2010. "TNF-A/NF-Kb/Snail Pathway In Cancer Cell Migration And Invasion". *British Journal Of Cancer* 102 (4): 639-644. doi:10.1038/sj.bjc.6605530.
83. Tang, Daofang, Detao Tao, Yuan Fang, Chao Deng, Qing Xu, and Jingping Zhou. 2017. "TNF-Alpha Promotes Invasion And Metastasis Via NF-Kappa B Pathway In Oral Squamous Cell Carcinoma". *Medical Science Monitor Basic Research* 23: 141-149. doi:10.12659/msmbr.903910.
84. Tanaudommongkon, Irin, Asama Tanaudommongkon, Priyanka Prathipati, Joey Trieu Nguyen, Evan T. Keller, and Xiaowei Dong. 2020. "Curcumin Nanoparticles And Their Cytotoxicity In Docetaxel-Resistant Castration-Resistant Prostate Cancer Cells". *Biomedicines* 8 (8): 253. doi:10.3390/biomedicines8080253.
85. Zuo Y, Zhu Z, Huang Y, Tao J, Li Z: Science of Chinese Materia Medica. A Newly Complied Practical English-Chinese Library of Traditional Chinese Medicine. Printed in Shanghai Xinhua Printing Works. 2003 ISNB 7 – 81010 – 682 – 1/R.624 p222-223.
86. Jiangsu New Medical College: Dictionary of Traditional Chinese Medicine. Edited by Nanjing University of Traditional Chinese Medicine. Shanghai Science and Technology Press, ISBN7-5323-0843-X. 2006. p1735-1737
87. Yang, Chunguang, Xueyou Ma, Zhihua Wang, Xing Zeng, Zhiquan Hu, Zhangqun Ye, and Guanxin Shen. 2017. "Curcumin Induces Apoptosis And Protective Autophagy In Castration-Resistant Prostate Cancer Cells Through Iron Chelation". *Drug Design, Development And Therapy* Volume11: 431-439. doi:10.2147/dddt.s126964.

88. Yang, Yong, Gening Jiang, Peng Zhang, and Jie Fan. 2015. "Programmed Cell Death And Its Role In Inflammation". *Military Medical Research* 2 (1). doi:10.1186/s40779-015-0039-0.
89. Ozaki, Toshinori, and Akira Nakagawara. 2011. "Role Of P53 In Cell Death And Human Cancers". *Cancers* 3 (1): 994-1013. doi:10.3390/cancers3010994.
90. Macleod, K F, N Sherry, G Hannon, D Beach, T Tokino, K Kinzler, B Vogelstein, and T Jacks. 1995. "P53-Dependent And Independent Expression Of P21 During Cell Growth, Differentiation, And DNA Damage.". *Genes &Amp; Development* 9 (8): 935-944. doi:10.1101/gad.9.8.935.
91. Database, GeneCards. 2022. "TMEM79 Gene - Genecards | TMM79 Protein | TMM79 Antibody". *Genecards.Org*. https://www.genecards.org/cgi-bin/carddisp.pl?gene=TMEM79.
92. "TMEM79 Protein Expression Summary - The Human Protein Atlas". 2022. *Proteinatlas.Org*. https://www.proteinatlas.org/ENSG00000163472-TMEM79.
93. Database, GeneCards. 2022. "ACOXL Gene - Genecards | ACOXL Protein | ACOXL Antibody". *Genecards.Org*. https://www.genecards.org/cgi-bin/carddisp.pl?gene=ACOXL.
94. Rory Stark, Marta Grzelak, James Hadfield. 2019. “RNA sequencing: the teenage years. *Nat Rev Genet”*. Nov;20(11):631-656. doi: 10.1038/s41576-019-0150-2. Epub 2019 Jul 24.
95. Miller, Anna K., Gloria Tavera, Ricardo L. Dominguez, M. Constanza Camargo, Tim Waterboer, Keith T. Wilson, Scott M. Williams, and Douglas R. Morgan. 2021. "Ornithine Decarboxylase (ODC1) Gene Variant (Rs2302615) Is Associated With Gastric Cancer Independently Of Helicobacter Pylori Caga Serostatus". *Oncogene* 40 (40): 5963-5969. doi:10.1038/s41388-021-01981-5.
96. Fattahi, Sadegh, Elham Ghadami, Mohsen Asouri, Ali Motevalizadeh Ardekanid, and Haleh Akhavan-Niaki. 2018. "Urtica Dioica Inhibits Cell Growth And Induces Apoptosis By Targeting Ornithine Decarboxylase And Adenosine Deaminase As Key Regulatory Enzymes In Adenosine And Polyamines Homeostasis In Human Breast Cancer Cell Lines". *Cellular And Molecular Biology* 64 (3): 97-102. doi:10.14715/cmb/2018.64.3.16.
97. Kaminski, Lisa, Stéphanie Torrino, Maeva Dufies, Zied Djabari, Romain Haider, François-René Roustan, and Emilie Jaune et al. 2019. "Pgc1α Inhibits Polyamine Synthesis To Suppress Prostate Cancer Aggressiveness". *Cancer Research* 79 (13): 3268-3280. doi:10.1158/0008-5472.can-18-2043.
98. Wise, David, Joshua Armenia, Yu Chen, Peter Nelson, Nikolaus Schultz, Charles L. Sawyers, and Howard I. Scher. 2017. "The Immunomodulatory Protein Dickkopf-1 (DKK1) Defines A Non-Neuroendocrine Subtype Of Metastatic Castration-Resistant

Prostate Cancer (Mcrpc) With Low AR And Low PSA Expression.". *Journal Of Clinical Oncology* 35 (15_suppl): 5054-5054. doi:10.1200/jco.2017.35.15_suppl.5054.

99. Chu, Hang Yin, Zihao Chen, Luyao Wang, Zong-Kang Zhang, Xinhuan Tan, Shuangshuang Liu, Bao-Ting Zhang, Aiping Lu, Yuanyuan Yu, and Ge Zhang. 2021. "Dickkopf-1: A Promising Target For Cancer Immunotherapy". *Frontiers In Immunology* 12. doi:10.3389/fimmu.2021.658097.
100. Guan, Yaoyao, Adheesh Bhandari, Xiaohua Zhang, and Ouchen Wang. 2019. "Uridine Phosphorylase 1 Associates To Biological And Clinical Significance In Thyroid Carcinoma Cell Lines". *Journal Of Cellular And Molecular Medicine* 23 (11): 7438-7448. doi:10.1111/jcmm.14612.
101. Wang, Chen, Ziyu Shi, Yuqian Zhang, Mingyue Li, Jie Zhu, Zhen Huang, Junfeng Zhang, and Jiangning Chen. 2021. "Cbfβ Promotes Colorectal Cancer Progression Through Transcriptionally Activating OPN, FAM129A, And UPP1 In A RUNX2-Dependent Manner". *Cell Death &Amp; Differentiation* 28 (11): 3176-3192. doi:10.1038/s41418-021-00810-2.
102. Tsai, Miaw-Sheue, Daphne F Bogart, Jessica M Castañeda, Patricia Li, and Ruth Lupu. 2002. "Cyr61 Promotes Breast Tumorigenesis And Cancer Progression". *Oncogene* 21 (53): 8178-8185. doi:10.1038/sj.onc.1205682.
103. Jeong, Dongjun, Suhak Heo, Tae Sung Ahn, Sookyoung Lee, Soyoung Park, Hyungjoo Kim, and Doosan Park et al. 2014. "Cyr61 Expression Is Associated With Prognosis In Patients With Colorectal Cancer". *BMC Cancer* 14 (1). doi:10.1186/1471-2407-14-164.
104. Terada, Naoki, Prakash Kulkarni, and Robert H Getzenberg. 2012. "Cyr61 Is A Potential Prognostic Marker For Prostate Cancer". *Asian Journal Of Andrology* 14 (3): 405-408. doi:10.1038/aja.2011.149.
105. Y-Z. Luo, P. He, M-X. Qiu. 2018. “FOSL1 enhances growth and metastasis of human prostate cancer cells through epithelial mesenchymal transition pathway”. *European Review for Medical and Pharmacological Sciences.* 22(24):8609-8615. doi: 10.26355/eurrev_201812_16624
106. Kubota, Kaiyu, Lindsey N. Kent, M. A. Karim Rumi, Katherine F. Roby, and Michael J. Soares. 2015. "Dynamic Regulation Of AP-1 Transcriptional Complexes Directs Trophoblast Differentiation". *Molecular And Cellular Biology* 35 (18): 3163-3177. doi:10.1128/mcb.00118-15.
107. Lukey, Michael J., Kai Su Greene, Jon W. Erickson, Kristin F. Wilson, and Richard A. Cerione. 2016. "The Oncogenic Transcription Factor C-Jun Regulates Glutaminase Expression And Sensitizes Cells To Glutaminase-Targeted Therapy". *Nature Communications* 7 (1). doi:10.1038/ncomms11321.

108. Jamnagerwalla, Juzar, Lauren E. Howard, Emma H. Allott, Adriana C. Vidal, Daniel M. Moreira, Ramiro Castro-Santamaria, Gerald L. Andriole, Michael R. Freeman, and Stephen J. Freedland. 2017. "Serum Cholesterol And Risk Of High-Grade Prostate Cancer: Results From The REDUCE Study". *Prostate Cancer And Prostatic Diseases* 21 (2): 252-259. doi:10.1038/s41391-017-0030-9.

109. Kaneda, Atsushi, Michio Kaminishi, Yukihiro Nakanishi, Takashi Sugimura, and Toshikazu Ushijima. 2002. "Reduced Expression Of Theinsulin-Induced Protein 1 Andp41 Arp2/3 Complex Genes In Human Gastric Cancers". *International Journal Of Cancer* 100 (1): 57-62. doi:10.1002/ijc.10464.

110. Lim, Syer C., Bekesho Geleta, Sanaz Maleki, Des R. Richardson, and Žaklina Kovačević. 2021. "The Metastasis Suppressor NDRG1 Directly Regulates Androgen Receptor Signaling In Prostate Cancer". *Journal Of Biological Chemistry* 297 (6): 101414. doi:10.1016/j.jbc.2021.101414.

111. Kochumon, Shihab, Amnah Al-Sayyar, Texy Jacob, Amal Hasan, Fahd Al-Mulla, Sardar Sindhu, and Rasheed Ahmad. 2021. "TNF-A Increases IP-10 Expression In MCF-7 Breast Cancer Cells Via Activation Of The JNK/C-Jun Pathways". *Biomolecules* 11 (9): 1355. doi:10.3390/biom11091355.

112. Tang, Daofang, Detao Tao, Yuan Fang, Chao Deng, Qing Xu, and Jingping Zhou. 2017. "TNF-Alpha Promotes Invasion And Metastasis Via NF-Kappa B Pathway In Oral Squamous Cell Carcinoma". *Medical Science Monitor Basic Research* 23: 141-149. doi:10.12659/msmbr.903910.

113. Wu, Y, and B P Zhou. 2010. "TNF-A/NF-Kb/Snail Pathway In Cancer Cell Migration And Invasion". *British Journal Of Cancer* 102 (4): 639-644. doi:10.1038/sj.bjc.6605530.

114. Zinatizadeh, Mohammad Reza, Bettina Schock, Ghanbar Mahmoodi Chalbatani, Peyman Kheirandish Zarandi, Seyed Amir Jalali, and Seyed Rouhollah Miri. 2021. "The Nuclear Factor Kappa B (NF-Kb) Signaling In Cancer Development And Immune Diseases". *Genes &Amp; Diseases* 8 (3): 287-297. doi:10.1016/j.gendis.2020.06.005.